Gaussian Process models for ubiquitous user comfort preference sampling; global priors, active sampling and outlier rejection.

Damien Fay[1], Liam O'Toole[2], Kenneth N. Brown[2].*

[1]*Faculty of Science and Technology, Bournemouth University, UK.*

[2] *Cork Constraint Computation Centre, Department of Computer Science, University College Cork, Ireland.*

Abstract

This paper presents a ubiquitous thermal comfort preference learning study in a noisy environment. We introduce Gaussian Process models into this field and show they are ideal, allowing rejection of outliers, deadband samples, and produce excellent estimates of a users preference function. In addition, informative combinations of users preferences becomes possible, some of which demonstrate well defined maxima ideal for control signals. Interestingly, while those users studied have differing preferences, their hyperparameters are concentrated allowing priors for new users. In addition, we present an active learning algorithm which estimates *when* to poll users to maximise the information returned.

Keywords:
Active learning, Gaussian process models, thermal preference, ASHRAE, PMV.

1. Introduction

Building energy consumption is a major factor in overall human energy consumption accounting for an estimated 20-40% of all energy consumption in the developed world [1], 43% in the US [2]. In addition, the trend appears to be increasing with this consumption in the EU rising at a rate of 1.5% each year; the rate of increase for less developed economies being far higher (4.2% in Spain for example) as their economies converge with the average [1]. Thus increase in building energy consumption has the potential to impact greatly on human energy consumption. A large part of this expenditure may be accounted for by HVAC systems (50% in the USA) designed to provide occupants with a comfortable working environment [1].

Occupant comfort is in itself an important factor effecting not just energy consumption but productivity, comfort, and the health of the occupants [3]. Indeed occupant behaviour, especially thermostat and ventilation flow usage was found to be a dominant factor in building energy demand prediction [4] outweighing structural quantities (wall conductivity, window parameters). It is important to note that an occupants comfort is a perception, *internal* to that occupant effected by, their clothing, their activity, their health and environmental factors. *External* environmental sensors alone are a poor estimator of that variable, however these are likely to remain the best measures available to us as sensing an occupants clothing index (for example) is overly intrusive. Finally, we may query the occupant themselves to get a measure of their comfort. Though a humans perception of thermal comfort is also a noisy estimator it has been found in a similar study that use of this information can yield up to a 20% saving in heating energy usage [5].

In order to assess an individuals perceived comfort level, we need to ask them how they feel. However, with the rise of ubiquitous computing individuals are now being bombarded by requests for attention and information from many sources (mobile phones, facebook, twitter etc.). As stated by York in a survey of Human Computer Interaction [6]; *Central to the concept of ubicomp* (ubiquitous computing sic.) *is that technologies should disappear*

*dfay@bournemouth.ac.uk

into the background so that users can unconsciously apply them to the task at hand. Thus there is a conflict; we need to ask the user how they feel but the interruption caused needs to be minimised. The interface design approach in this research minimizes the interaction with the user but this comes at a cost; users do not consider at length how they feel about their comfort; thus the data collected contains a lot of noise and artefacts. It is an aim of this paper to show how user preferences can still be extracted from data in the presence of such measurement noise. In order to further minimise interaction with the user we examine an active learning paradigm. Under this paradigm the user is polled for their perception only when the expected information returned maximises the information about their comfort function. To paraphrase, their is no point asking a user if they feel uncomfortable at say 21° C if prior evidence already suggests they are.

The specific statistical approach used in the study is based on Gaussian Process (GP) Regression. While involved, the GP approach solves the aforementioned problems allowing a good estimate of a users preference function. In addition, a GP approach allows for extra functionality which we investigate. Specifically, we show how the GP estimates may be used in a natural way to combine the preference functions of individuals sharing the same office space. Also the GP estimates can be used in an online manner to estimate when is the best time to collect a sample (active learning).

The scenario thus described is represented in Figure 1. In our study we measure the environmental variables *at the desk* of each participant and the external weather conditions. Using these and previously measured user thermal preferences as input an individual model of user thermal preference is constructed. Note that there are two feedback loops in the overall system, one from the environment to the controller with the setpoint dynamically determined by a module which combines the preferences of all occupants. The second loop is from the environment to the user model with the active learning module acting as a controller to select the best time to ask the user for their preference. Finally, note that this research looks at all aspects of this scenario except the control loop which will be examined in future research.

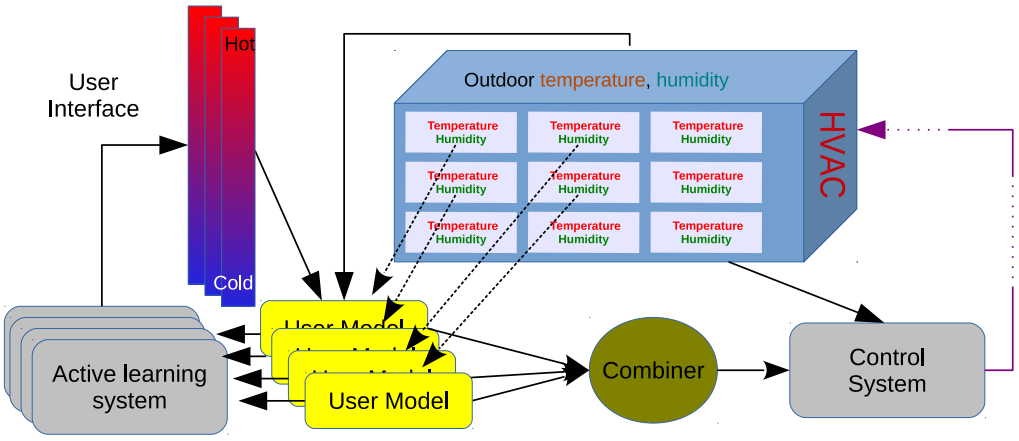

Figure 1: Overview of control and measurement environment.

In our prior research [7] we examined a Gaussian Process model based on the raw response data alone and a single combination of those predictions. In this paper we extend that research by comparing that model with two alternate models. In addition:

- We examine 4 methods for combining the preferences of several individuals based on maximising the expected neutral vote (Section 5.3.2),
- We examine the suitability of different combination strategies as control signals,
- We show empirically that all humans share a common set of hyper-parameters,
- We show how this can be used as a prior to give new users a reasonable model and also which improves the active learning control loop (Section 5.3.1), and

- We show that with active learning (incorporating prior information) a typical user may need as little as 15 samples to obtain a reasonable fit of their thermal preference model (as opposed to 20 measurements for a random approach) (Section 5.4).

2. Related Work

With reference to Figure 1 much of the previous work in this area has tended to view the user as the average human being and so the entire active feedback loop is replaced with an open loop lookup table. These tables are derived typically from the ASHRAE standard [8][9] which defines thermal comfort using the *Predicted Mean Vote* (PMV) [10] and associated Predicted Percent of users Dissatisfied (PPD). In order to fully estimate these quantities one must also measure the clothing index, metabolic rate, gender, and other factors which are not possible in a ubiquitous environment [11] (see [12] for a indepth study which does identify factors which would be appropriate for ubiquitous systems to measure).[1] In addition, a recent study has proposed that the PMV is now a biased estimate of the average users preference in many regions of the world [13]. Further approaches seek to dynamically adjust the setpoint using measured environment variables but all without a human feedback mechanism [14] [15] [16]. One recent notable approach uses Bayesian probit analysis to map PMV and environmental measures to sensation, acceptability and preference [17] providing a deeper understanding of human perception of their environment.

Model driven approaches which model individual preferences based on feedback can be found in several papers [11][18][5] and some commercial systems such as the *Comfy* system from BuildingRobotics[2]. In particular it has been stated that Building Management Systems' (BMS) operators tend to set conservative setpoints (to avoid complaints) leading to wasted energy. [5] estimated in simulations an 18% reduction in energy usage by using models for individual users, while [19] cites a 10% improvement.

Feedback from occupants has long existed in the form of thermostats but in a multi-occupant scenario this can lead to conflict and in addition, the fact an occupant is using a thermostat indicates the environment is intruding on their work. *Thermovote* [19] is an application using smart devices which measure feedback from users which are combined to control office environments. The system differs from that examined here in that user preferences are combined with equal weighting and the approach is not model driven (a users preference is used immediately in a voting pool to adjust the environment). Daum et. al. [18], discusses the conflict between different users preferences noting the diversity of preferences and problems faced when trying to combine them into one function with a well-defined peak. Song et. al. [20] present a system with a similar aim to that here which learns user preferences and combines them for use in the BMS system. While our approach allows combination of preferences and active learning as in [18][20], it differs in that we use a purely Bayesian approach based on the what the samples themselves reveal rather than assuming a model for the data a priori;[3] a functional logistic model relationship in [18] or using a collaborative rule engine in the case of [20]. Zhao et. al. [21] proposes two zones, a comfort and discomfort zone and recursively estimates the boundary set between these.

In an early paper (1989), Cass and Steffy [22] discuss conditionally independent hierarchical model (CIHM's). A CIHM is a Bayesian hierarchical model for several processes which have different parameters but a common set of hyper-parameters. These models are common in the real world including across animals, humans and cities etc [22]. In the current setting, a CIHM for user preferences would imply each users preference (process) is different but that the hyper-parameters used to construct the preferences are common. We present empirical evidence that the GP's used here are in fact CIHM's; i.e. humans share a common structure in the second level of the hierarchy (see Section 5.3.1). Daum [18] similarly uses global priors so that new users will have a profile even though they may not have yet donated any samples. These profiles are then updated as new measurements arrive as is examined in this research.

Active learning of user preference functions has not to our knowledge been examined widely in academia, though several commercial thermostats exist which seek to learn user behaviour [23]. Active learning differs however in that the aim is only to poll the user when the information returned is useful (above a threshold or according to some constrained budget). To the best of our knowledge is it novel in the area of thermal comfort modelling but has a long

[1] In our models we use the internal room temperature, the external (outdoor) temperature and the internal room humidity as these can be easily and non-intrusively measured.

[2] http://buildingrobotics.com/comfy

[3] We do however test if using the PMV predictions as a prior is beneficial for the Bayesian model.

history and has been applied in many fields such as robot control [24], fault detection [25], as a general optimization approach [26] amongst others [27][28][29].[4].

3. Interface and data collection procedure.

The design of a user interface for preference modelling can have a significant effect on the quality of the data returned as was examined in [11]. They tested several different interfaces and also noted that the more accurate the measurement the greater the attention/annoyance required from the user. In this study we seek to cause as little intrusion as possible and so our interface is designed to be a one-click interface. The interface conveys the scales via colour (blue for cold and red for hot) and Figure 2 shows a cropped screenshot in which the user interface appears in the top left corner of the user's computer screen.

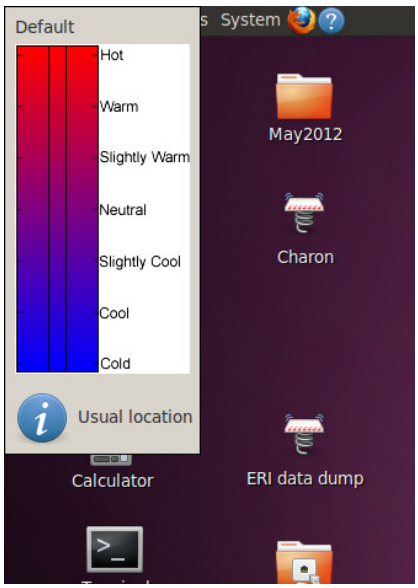

Figure 2: A cropped screenshot showing the user interface (top left corner).

As can be seen there is a colour bar, with the 7 Ashrae standard labels to the right of the colour bar (hot, warm, neutral etc.). There are also two vertical lines in the centre of the colour bar which are called the *validation lines*. The user is instructed to click between the validation lines at the appropriate colour using the labels on the right as a guide. In addition, the user has been asked that in the event they are busy or engaged or just not interested they should click outside the validation lines in the area where the labels reside (see Section 5.1 for a discussion of this feature and the *deadband*). Once a click has been received the interface disappears and does not appear again for several hours (there are a maximum of three samples times each day chosen randomly but the user might not respond or be present). The deviation from neutral is the dependent variable in the model, Y, and lies in the *continuous* range $[-3, 3]$ which corresponds to the Ashrae scale {Hot = 3, Warm =2, ..., Neutral = 0, Cold = -3}.

To avoid catching the user just after they have entered work (in which case they are not yet acclimatised to the environment) a delay is incorporated; the interface is only shown ten minutes after a (any) click has been received on the computer, the aim being to avoid polling within 10 minutes of a users entry.

Although the labels in Figure 2 correspond to the ASHRAE labels there is an important difference; the ASHRAE polls consists of 7 discrete levels, the polls taken here are continuous. This allows us to take an exact measurement and thus avoid quantisation error.

The preference collection software was rolled out in three different sites. Table 1 gives a summary of the data collected in this study and Figure 3 shows the number of samples collected, for each site, every day. In addition, the prevailing weather and the room temperatures across the survey are shown. The first is at a room in University College Cork (UCC) in which each user has a temperature and humidity sensor located at their desk. This site is the most important in terms of instrumentation and control but contains the least number of participants; just four. The HVAC system consists of underfloor storage heating (commonly used in regions with cheap night-time electricity rates) and natural ventilation; the room also has a large south facing window. The environment is difficult to control (as there is a lag of approximately eight hours between the control/storage heating and the resulting temperature in the room); this site presents the largest variation in the environment. These users will be used as the main group for the discussion in the results.

The second implementation was in a research building at Cork Institute of Technology (CIT). There are 21 participants located in 7 different rooms; all with East or West facing windows. These rooms have been fitted out with temperature sensors in various locations and for the 21 participants there are 13 sensors. The HVAC system here is modern and has been in usage for several years and so the environment here showed the least amount of variation.

[4] gaussianprocesses.org is also a good resource for the interested reader.

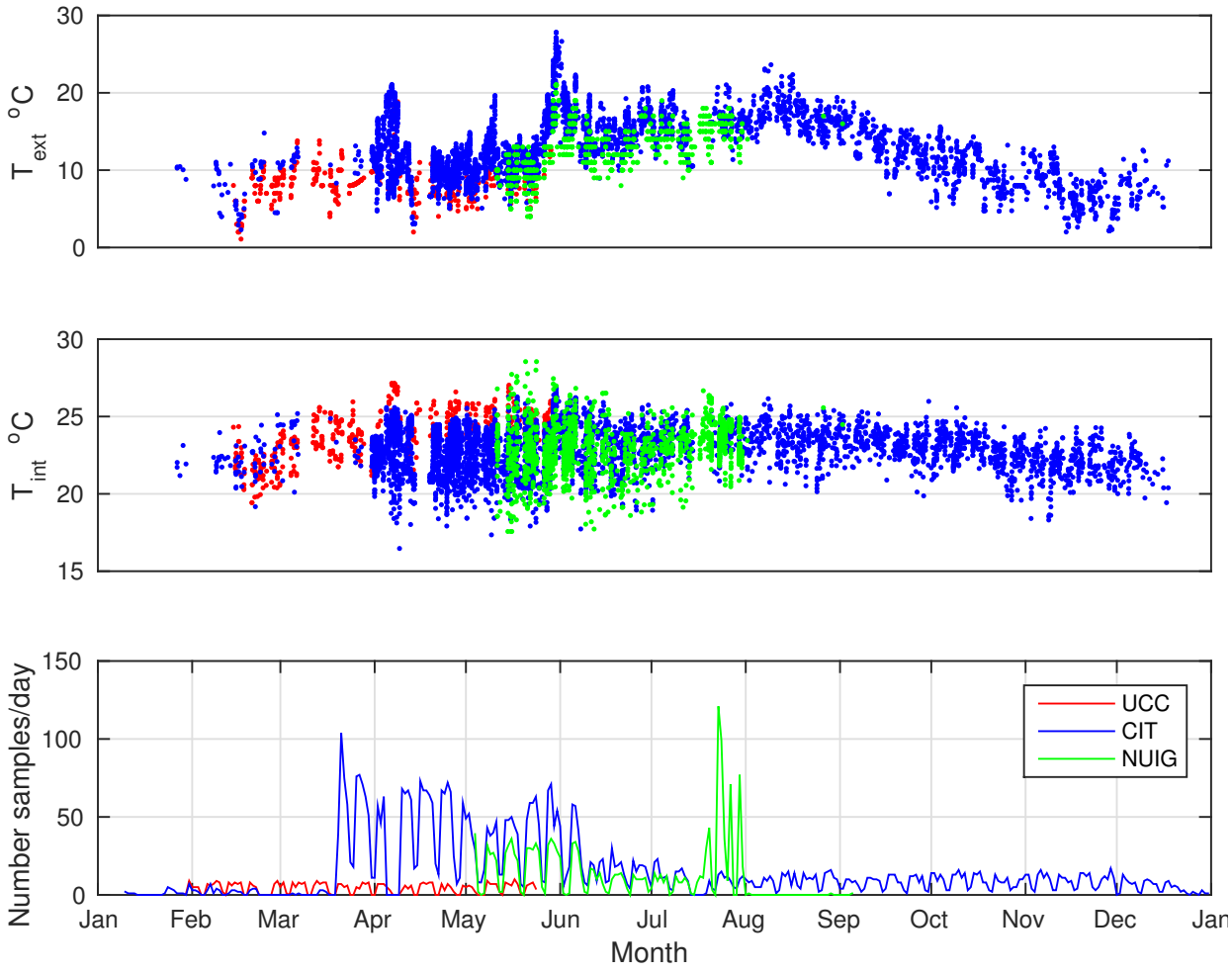

Figure 3: External and Internal temperature, and the number of samples collected per day at the three sites.

The third implementation took place in the New Engineering Building at NUI, Galway. This building contains two elongated Ph.D rooms each containing space for one hundred students. The rooms are south facing, the HVAC system employs a combined heat and power unit and the windows are darkened to reduce solar glare. [5] The UCC participants are all Irish males aged 35-45, The CIT population consisted of postdoctoral researchers aged in the region of 35. The NUIG population consisted of PhD students from diverse international backgrounds mostly aged in their mid to late twenties. All three rooms are research offices where the occupants spend most of their time seated at their desks.

In addition to the sensors located at each site weather information in the form of the external prevailing temperature was available as samples taken hourly. In addition, the external humidity was measured but was not found to be a major factor in preference learning.

4. Gaussian processes and active learning

The preference modelling domain has particular characteristics. Here we enumerate these and later in this and other sections we indicate how those characteristics are considered by the model:

[5] This building was designed as 'living laboratory' and won several awards for its innovative design. More details may be found on the buildings webpage http://www.nuigalway.ie/new-engineering-building/greencredentials/.

Site	Number Participants	Average number of polls (Max,Min,Std)	Mean duration (days)	Average samples per day (Max,Min,Std)	Internal Temperature	Internal Humidity	External Temperature	Environment
UCC	4	38 (61,14,20)	128 (159,67,41)	0.83 (0.98,0.48,0.23)	Yes	Yes	Yes	Controlled, large variation.
CIT	21	65.5 (189,5,39)	74.1 (277,4,54.6)	1.4 (5.3,0.30,3.4553)	Yes	No	Yes	Controlled and tuned.
NUIG	53	98.5 (227,11,54)	169 (306,9,89)	0.5095 (1.66,0.4,0.32)	Yes	No	Yes	Controlled and tuned.

Table 1: Summary of data collected.

$C\mathbf{1}$: There are numerous factors that influence somebodys preference which we cannot measure (without being overly intrusive), such as their clothing or their awareness of their comfort (discussed in Section 1). This leads to measurement noise and this noise can be excessive leading to *outliers*,

$C\mathbf{2}$: The noise is heterogeneous. Some parts of the input space will have a higher expected variance than others. For example, a neutral vote is particularly suspect due to the demand characteristic (Section 5.1),

$C\mathbf{3}$: Samples are not evenly distributed. We sample an environment that a system (the HVAC) is deliberately trying to make comfortable; i.e. it is attempting to force all the samples to come from a narrow region of the input space,

$C\mathbf{4}$: Prior information is available. Comfort modelling has been considered important for a long time and there is wealth of research already conducted into this area and so there is *prior information* available which could benefit the models,

$C\mathbf{5}$: Multiple occupancy of space. Rooms are typically occupied by several people and a combined preference is required in this case, and

$C\mathbf{6}$: Samples are intrusive to collect. Finally, as stated in the introduction we view polling a user as an interruption. As will be shown Gaussian Processes are perfectly suited to addressing the six characteristics cited above in a single framework.

4.1. Gaussian Process Models

A *Gaussian Process* (GP)[6] is a modelling framework that primarily looks at the shared information between samples. For example, we might accept that a participants comfort level at say 23°C tells us a lot of information about their preference at 23.1°C, but, perhaps not so much at 35°C. How do we quantify that shared information? A GP assumes that the information/correlation between samples is dependent on their distance apart, that dependency being made specific by a function of distance called the *kernel function*. If we take several samples together then we can combine them to estimate the value of the function at an unknown point where that combination is based on the distance from that point to the known samples/information. In addition, we may estimate the parameters of the model by optimising how well they predict each others values. There is no restriction on the distribution of samples ($C\mathbf{1}$), a GP will simply combine whatever information it has been provided, thereby predicting at any location in the input space. Crucially it will also provide an estimate of that prediction variance. The specific details of the GP employed here are now presented.

A GP consists of assigning a kernel to each measured data point and performing a regression based on that kernel and the measurement noise at that data point. In the following we summarise the theory behind this Gaussian Process model and the interested reader may find more detail in [7]. Given an d dimensional input, $x \in \Re^d$, the data is first scaled such that the variation in all dimensions along the data is the same. To achieve this the data is typically multiplied by a scaling matrix $M \in \Re^{d\times d}$. There are several choices for M [30] including a factorial analysis form but that chosen here is to have M as a diagonal matrix. [7] M thus consists of d elements and we choose to keep the first entry on the diagonal as 1. The reason for this choice is that the first variable is internal (building) temperature, the dominant variable, which is already in units that can be easily interpreted. Thus M consists of $d-1$ *unknown* elements denoted, $\{m_1, \ldots, m_{d-1}\}$. These unknowns can be incorporated into the set of hyperparameters for the GP; the estimation procedure is discussed below.

A GP is defined as a process in which realisations from the process are jointly multivariate Normally distributed. Specifically, the data generated by the process at n sample points, $Y_{x_{1:n}}$, are drawn from a multivariate Gaussian

[6] An excellent primer for GP's may be found in [27].

[7] The reason is that the inputs involved; internal temperature, external temperature and internal humidity can reasonably be thought to be independent due to HVAC control; even the internal humidity is controlled separately from the internal temperature by the outside air intake valve.

distribution as:

$$Y_{x_{1:n}} \sim \mathcal{N}[\mu_x, C_{\mathbf{x},\mathbf{x}}] \tag{1}$$

where $\mathcal{N}$ denotes a Gaussian distribution, $x_{1:n}$, denotes n samples taken at points $x_1 \dots x_n$, $\mu_x \in \Re^d$, is the mean of the process and $C_{\mathbf{x},\mathbf{x}}$ is the covariance matrix, and $\sim$ denotes drawn from. Following appropriate scaling of the inputs (discussed below) an **isotropic** covariance matrix can be used in which the variation of the function is equal in all directions. Given an isotropic covariance function it now becomes more convenient to talk in terms of the correlation function which is related to the covariance function via[8]:

$$C_{\mathbf{x},\mathbf{x}} = \sigma_x^2 R_{\mathbf{x},\mathbf{x}} \tag{2}$$

as σ_x^2, is the variance of the process and $R_{\mathbf{x},\mathbf{x}} \in \Re^{n \times n}$ is the correlation function.

In this application, a monitonically decreasing kernel is apt as one expects similar environments to provide similar comfort levels. However, it is unclear just how far knowledge at one point in the input space extends. For that reason the Matérn Kernel, derived from the t-distribution is used as this kernel can take on a variety of shapes; from a Gaussian-like shape, to shapes peaked at zero *and* with a long tail. In addition, it has only two parameters. The Matérn kernel is defined as:

$$R(h, \theta, \nu) = \frac{1}{\Gamma(\nu) 2^{\nu-1}} \left(\frac{2\sqrt{\nu}|h|}{\theta} \right)^{\nu} K_\nu \left(\frac{2\sqrt{\nu}|h|}{\theta} \right) \tag{3}$$

where K_ν is the modified Bessel function, θ and ν are parameters of the kernel with θ controlling the scale and ν the shape of the kernel.

Now, given a set of points at which samples have already been taken, $x_{1:n}$, and a set of locations (called evaluation points), x^*, at which we have not sampled, the relationship between the sampled and evaluation points may be expressed by partitioning Equation 1 in terms of the cross and auto-correlation matrices of the sampled and evaluation points as [27][9]:

$$\begin{bmatrix} Y_{x_{1:n}} \\ Y_{x^*} \end{bmatrix} \sim \mathcal{N} \left[\begin{bmatrix} \mathbf{1_n} \\ \mathbf{1}_* \end{bmatrix} \mu_x, \sigma_x^2 \begin{bmatrix} R_{\mathbf{x},\mathbf{x}} & R_{\mathbf{x},x^*} \\ R^T_{\mathbf{x},x^*} & R_{x^*,x^*} \end{bmatrix} \right] \tag{4}$$

where Y_{x^*} is the value of the process at x^*, $\mathbf{1_n}$ and $\mathbf{1}_*$ are appropriately dimensioned vectors of ones, $R_{\mathbf{x},\mathbf{x}}$ is the auto-correlation between the known sample points, $R_{\mathbf{x},x^*}$ is the cross-correlation between the sample and evaluation points and R_{x^*,x^*} is the auto-correlation of the evaluation points.

The set of unknown parameters for the GP model is $\{\mu_x, \sigma_x^2, \theta, \nu, m_1, \dots, m_{d-1}\}$. These may be estimated iteratively using Bayesian conjugate analysis and a hierarchical GP in which the parameters are organised in a hierarchy as:

$$[\mu_x, \sigma_x^2, \theta, \nu] = [\mu_x | \sigma_x^2] \times [\sigma_x^2] \times [\theta, \nu, m_1, \dots, m_{d-1}] \tag{5}$$

where $[\bullet]$ denotes distribution. It is thus assumed that the kernel and data scaling parameters are independent of the process mean and variance and may be estimated first followed by the next stage in the hierarchy; estimating the variance and then the process mean (conditional on the variance). Finally, estimates of the function at particular sample points may be made given the hyperparameters. $[\theta, \nu, m_1, \dots, m_{d-1}]$ can be estimated by maximising the log marginal likelihood as [30]:

$$L = -\frac{1}{2} Y^T_{x_{1:n}} C^{*-1} Y_{x_{1:n}} - \frac{1}{2} log|C^*| - \frac{n}{2} log(2\pi) \tag{6}$$

where $L \equiv \log p(Y_{x_{1:n}} | x_{1:n}, \theta, \nu, m_1, \dots, m_{d-1})$ is the log likelihood function, $C^* = \sigma_x^2 (R_{\mathbf{x},x^*} + \zeta_x)$, is the covariance matrix of the noisy data and ζ_x is the measurement noise covariance.[10]

The process parameters are estimated using a conjugate Bayesian approach in which the standard conjugate Bayesian prior for a mean and (unknown) variance are used; specifically the mean has a normal prior; $\mu_x \sim \mathcal{N}\left[0, \sigma_x^2 \delta^2\right]$ and the variance has a normal-inverse-Gamma prior; $\sigma_x \sim \mathit{IG}\,[a/2, b/2]$. δ is our initial estimate of the variance of the mean, the variance is initially assumed to lie in the interval $[a, b]$.

[8] Here is assumed that the overall process mean is zero; alternatively a non-zero mean may be subtracted from the data prior to modelling.

[9] This Equation allows us to estimate the model at any point while accounting for the distribution of the samples in the input space; *C*3.

[10] Note: it is assumed that the noise is heterogeneous [31][32] as will come in useful in the results; Section 5.

An estimate of the function at the evaluation points may be constructed using least squares (see [27] for details). However, in the current application we are interested in estimating the value of Y_{x^*} given that the measurements are noisy. In the presence of measurement noise Equation 4 becomes [30]:

$$\begin{bmatrix} Y_{x_{1:n}} \\ Y_{x^*} \end{bmatrix} \sim \mathcal{N}\left[\begin{bmatrix} \mathbf{1_n} \\ \mathbf{1}_* \end{bmatrix} \mu_x, \sigma_x^2 \begin{bmatrix} R_{\mathbf{x},\mathbf{x}} + \zeta_x & R_{\mathbf{x},x^*} \\ R^T_{\mathbf{x},x^*} & R_{x^*,x^*} \end{bmatrix}\right] \tag{7}$$

and an estimate of the value of the function at the evaluation points, x^* may be expressed as [30]:

$$\hat{Y}_{x^*} = \mathbf{1}_* \hat{\mu}_x + R_{\mathbf{x},x^*} \left(R_{\mathbf{x}} + \zeta_x\right)^{-1} \left(Y_{x_{1:n}} - \mathbf{1_n}\hat{\mu}_x\right) \tag{8}$$

An estimate of variance at the evaluation points, $\sigma^2(x^*)$, may be estimated via [30]:

$$\hat{\sigma}^2(x^*) = \hat{\sigma}_x^2 \left(R_{x^*} - R^T_{\mathbf{x},x^*} K R_{\mathbf{x},x^*} + \frac{\left(1 - \mathbf{1_n}^T K R_{\mathbf{x},x^*}\right)^2}{\mathbf{1_n}^T K \mathbf{1_n} + \delta^{-2}} \right) \tag{9}$$

where $K = (R_{\mathbf{x},\mathbf{x}} + \zeta_x)^{-1}$ is used to simplify notation. Note that it is through ζ_x that $C\mathbf{1}$ and $C\mathbf{2}$ may be considered in the model. The maximum a-posteriori estimates for the process parameters are [24]:

$$\hat{\mu}_x = \left(1 - K + \delta^{-2}\right)^{-1} \mathbf{1_n}^T K Y_{x_{1:n}} \tag{10}$$

and

$$\hat{\sigma}_x^2 = \frac{\left(b + Y^T_{x_{1:n}} K Y_{x_{1:n}} - (\mathbf{1_n}^T K \mathbf{1_n} + \delta^{-2})\right)\hat{\mu}_x^2}{n + a + 2} \tag{11}$$

4.2. Outlier influence reduction.

At this stage the base model has been presented but there still remains one set of unknowns in the equations above, the measurement noise at the sample points, ζ_x. In many cases this is assumed to be constant [30] or another GP is employed to model the variance in addition to the mean (see [31] [32]). However here we use an approach similar to that in [29]. This approach assigns a different variance to each data point and can be used to reduce the effect of outliers (by assigning a higher variance to those points); this contrasts with other approaches which exclude outliers entirely which is problematic as there is no fixed definition of an outlier. In the current setting, an initial guess can be made for the variance of a sample/poll (see Section 5.2.2), say ζ_x^0. Given this initial guess the GP can be used to produce an estimate of the process at x, i.e. $\hat{Y}_x$, and this can be taken from the measured value to produce a residual. A recursive procedure can then be used to further estimate the variance based on the residual as ($C\mathbf{1}$):

$$\zeta_x^i = \alpha \zeta_x^{i-1} + (1 - \alpha) r_x^i \tag{12}$$

where $r_x^i = \hat{Y}_x - Y_x$ is the residual at x in iteration i and α is a coefficient which is here set to 0.7 (although this algorithm was found to be robust to different values of α). The net effect of this algorithm is that outliers are excluded as demonstrated empirically in Section 5.2.1.

4.3. Active Learning.

Active learning is a recursive procedure in which an estimate of a process, based on current data, is used to inform on the best point to sample the function at next. The process is then sampled at that point and the process estimate is updated and so on recursively (this Section deals specifically with $C\mathbf{6}$). Active learning is appropriate when the number of samples that can be taken is limited due to time or cost or, in this case, nuisance to the user. Thus, it is important to maximise the information gained from each sample. Examples of active learning with GP's may be found in [33][34][35]. Active learning is implemented in several stages, each of which must be tailored to a particular application:

(*i*) *A model* for the data which also specifies the confidence of the model; in this case we employ a hierarchical Gaussian Process model for regression (i.e. noisy measurements) in the presence of heteroskedastic noise as explained above,

(*ii*) A function which takes the mean and variance estimates and converts these into a value representing the expected return *if* we were to sample at that point. This is known as the *infill function* (see Section 4.4). In this case the *expected return* is the improvement of the estimate of the *entire function*, and

(*iii*) The maximum value of the infill function is estimated and used to select the location of the *next sample*. This current application is somewhat different from the standard setting in that the set of possible locations at which the function can be sampled at are not under our control. Given the environmental conditions (or estimates of them) for the day ahead, the algorithm must determine at what time it is optimal to sample at. We will call this set of environmental conditions a *path* as it is essentially a single path through the input space that takes place in the course of a day. The aim is to find the point on that path for which the information returned is a maximum.

4.4. Infill Function

The role of an infill function is to estimate the *expected return* from sampling at a particular point. In terms of approximating a function, there are two commonly used infill functions; the entropy approach proposed by MacKay [36] and the squared error approach suggested by Cohn [37]. In the entropy approach the expected return is the information gained about the GP parameters by sampling at a candidate point [36]. This in fact corresponds to sampling at that point which has the highest sample variance [36], $\hat{\sigma}^2(x^*)$, which is immediately available from the GP. In the squared error approach, the expected return is the average reduction of estimate variance across the entire function. The squared error approach is often preferred as the entropy approach tends to be maximised at the boundary of a function.[11] The squared error approach can be costly however, as it requires evaluating the entire function over a fine grid for every candidate sample (the computations required for the entropy approach are part of the GP algorithm already). In this case we are not free to select the input candidate points; the candidates are the input *path* and so the boundary issue does not arise. The entropy approach is thus preferred in this setting.[12]

5. Results

The results are broken into four major sections; the first presents a preliminary analysis of the data demonstrating major characteristics (5.1). The aim of the second section is to show the GP models in operation and does so by presenting the results from a single user (5.2). The third section validates the models and presents group results from the three sites and combining preferences (5.3). Finally, active learning is given its own Section (5.4).

5.1. Preliminary data analysis

When a user is busy and just wants to remove the interface three events can occur: i) They could click outside the validation lines (as instructed), the location of their click being thus irrelevant, ii) they might alternatively click inside the lines but at a random location (in which case they will generate an outlier in the data), or iii) they might click at the centre of the interface. The data presented below shows us that event i) did in essence not happen (only 2% of all clicks are outside the validation lines), ii) there are definitely outliers in the data (see Section 4.2) although they may be caused by other factors and iii) does occur quite often (23% of all samples) but many of these are also a neutral vote. Figure 4 shows three specific examples which encompass the behaviour seen by all users. Figure 4a comes from a typical user; almost all the responses are between the validation lines (in blue), some indicate it is too hot while others indicate it is too cold, and there is a cluster of responses around zero which indicate a neutral opinion. Figure 4b shows the responses of a user who misinterpreted the instructions and clicked instead on the ASHRAE labels; note that for this user there is not a large concentration of points around zero/neutral, i.e. this user does not exhibit a deadband. Seven users misunderstood the instructions and clicked on the ASHRAE labels instead of the colour bar; however as the users intention is still clear (if they clicked near the label 'HOT' then this provides the same information as them clicking on the red colour), this data was accepted for modelling. It was found that these models produced similar forecast variances to the rest. Figure 4c shows the responses of a user who appears to be too cold most of the time. Again there is no obvious deadband for this user. Next we examine the deadband in more detail.

[11] Intuitively, a point in the interior of the search space may have samples to its right and left (in 1-D) and thus will be expected to have a lower variance than points on the boundary. Thus the bias in the infill function in [36]. See [28] and [29] for a more in depth discussion.

[12] See [38] for an example where the squared error approach is preferred.

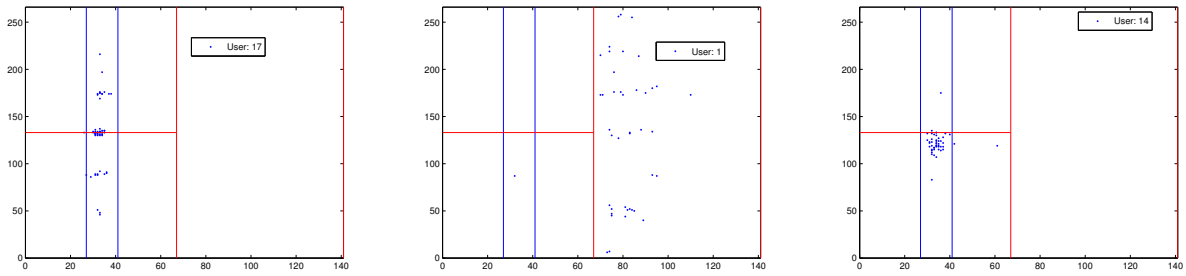

(a) All responses between the validation lines. (b) Clicked on the ASHRAE labels by mistake. (c) A User for whom the environment is always too cold.

Figure 4: The responses from 3 users: (a) Typical, (b) Misunderstood, and (c) No deadband.

Figure 5a shows the responses of a typical user with respect to the internal temperature (note that there are other dimensions to the data not shown here). As can be seen the relationship between internal temperature and the deviation, Y is quite cluttered and there appears to be a band around $Y = 0$ for which the response is invariant to the input; the aforementioned deadband.

The Gaussian Mixture model (GMM) [39] function in matlab is used for cluster detection under the assumption of three clusters one at $Y = 0$ (the deadband), one at $Y = -0.7$ and one at $Y = +0.7$ (the latter two being nuisance clusters used to assign non-deadband data). The resulting deadband is shown in Figure 5b and shows a clear band of entries from 21 to 26 °C for which the user gave a near zero response. The likely causes of this deadband are several fold; some are expressions of genuine comfort. However, others may come from the *demand characteristics* [40] of the poll, that is, participants have a tendency to answer what they believe the questioner wants to hear, in this case that they are comfortable. It was found that very few clicks occur outside the validation lines; i.e. users are not using this feature to indicate that they don't care to answer the poll at this time. Anecdotally users indicated that when they didn't care they usually clicked at the neutral position. In addition, even though a user may be too warm/cold when polled they might not be aware of that fact as the skin is a very bad at perceiving warmth and cold [41] especially when the room heats up slowly [13] and so click again at the neutral position. Statistically the deadband constitutes a *different process* which should either be taken out of the data altogether or discounted during modelling. Note that for approximately half of users a deadband does not exist. Given a 'deadband' from the GMM it may be tested to see if the centre of the band is statistically different from zero using the usual t-test. This was found to be a robust way of detecting the presence or not of the deadband for all users.

Figure 5c shows the same data as in Figure 5b but this time with the deadband removed. The relationship between internal temperature and Y is now somewhat clearer. Indeed a simple linear model (shown in Figure 5c), created purely for illustration purposes (the actual model is a GP), shows a reasonable fit to the data; this model implies that this users optimal internal temperature is in the region of 24°C; a plausible result. Given the preliminary elimination of the deadband data a more complex models based on Gaussian processes may now be constructed.

5.2. Operational results.

5.2.1. Gaussian Process models.

In this section we propose and contrast 3 different Gaussian Process models:[14] The first model, *GP1*, is a pure GP model (as described in Section 4) which models the relationship between the input and output using a Matern kernel. The second, *GP2*, is a *regressive GP* model [30], the aim of which is to use the PMV model as prior information ($C4$; i.e. we shall incorporate the average response of a human being a guess to which the estimates will tend in the absence of contrary information) in which the PMV is removed from the data prior to modelling; thus this model predicts the

[13] A well known example is the urban legend about boiling a frog slowly; due to the slow change in temperature the frog will not notice until its too late.

[14] In [7] only model 1 was explored.

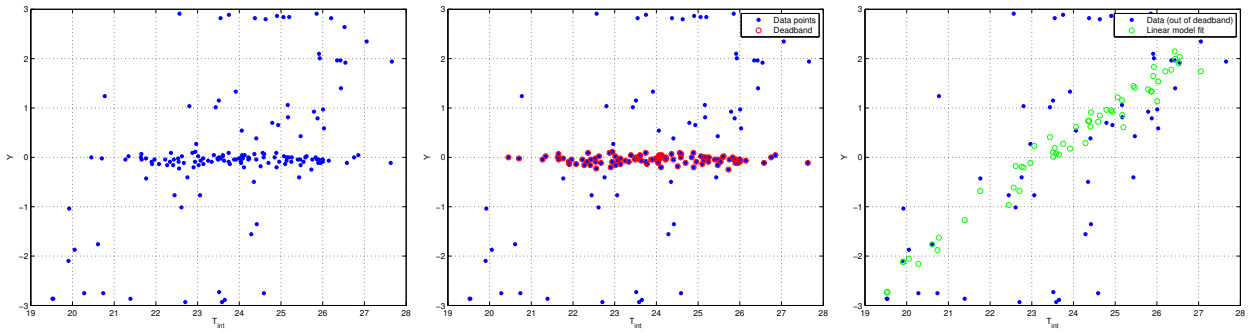

(a) (b) (c)

Figure 5: The deadband of a user: (a) Raw data, (b) Deadband identification, and (c) Deadband removal and a linear fit.

deviation from the PMV (i.e. $Y_{x_{1:n}} \sim \mathcal{N}[\mu_x - Y^{PMV}_{x_{1:n}}, C_{\mathbf{x},\mathbf{x}}]$) . The third model, *GP3*, is a regressive model with offset. This model predicts the deviation from the PMV and assumes that for each user there is an unknown fixed bias (for example, a preference may tend to be consistently 1° higher than that predicted by the PMV (see [13])). We introduce this offset by changing the kernel from a Matern kernel (4.1) to a Matern kernel summed with a constant, Δ as:

$$R'(h,\theta,\nu) = \frac{R(h,\theta,\nu) + \Delta}{1+\Delta} \tag{13}$$

where the denominator ensures $R'(0) = 1$.

We now begin by looking at how the input space is scaled by the fitted models. Figure 6a shows the original *input* data for a single sample user (using GP1); the internal temperature, the internal humidity and the external temperature. The original data shows that the internal temperature spans a lower range than the external temperature; it is unclear how humidity is related to the temperatures as it is in a different unit (percentage). The Maximum Likelihood Estimates (MLE) for the scaling parameters (Equation 6) are $m_{T_{ext}} = 2.68$ and $m_{H_{ext}} = 0.62$.

Figure 6b shows the input data for this user after input scaling. Comparing this with Figure 6a one can see that the external temperature has in fact been expanded (by a factor of 2.68) while the Humidity has been compressed, i.e. the scales have changed quite significantly. By expanding the external temperature scale the effect of each external input point becomes more localised (the kernel covers less of the range). Conversely, the humidity has been compressed and the kernel is quite wide in comparison to the range of the scaled humidity. Thus each humidity reading has a global rather than local effect on the estimate of the function. The kernel itself is shown alone in Figure 9; the kernel parameters being $\{\theta = 2.91, \nu = 2.54\}$ (Equation 6). The kernel has a value of 0.5 at a distance of 2 degrees and dies away quite slowly. The results are similar for GP2 and GP3.

Next we examine the predicted response for User 1 from the three models. As the input space is three dimensional this is presented in 2-D by holding some of the inputs constant. In Figure 7 the fit from the three models can be observed. The first thing to note is that the fit from GP1 is quite different from that of GP2 and GP3 (as we will see later the predictive power of all 3 models is however comparable). GP1 deviates significantly from the PMV at high/low temperatures (this is most evident in Figure 7a) as there are insufficient samples in these regions. Given no information a GP will regress to the process mean (~ zero). However, this should not be considered a deficiency in the model. As can be seen in Figure 7d (lower panel), the predictive variance for the model rises sharply outside [22°-26°] reflecting the lack of samples outside this range. Thus the model readily indicates when estimates are accurate and when they are not.

Figures 7(d-i) show the fits obtained from GP2 and GP3. These model the deviation from the PMV and so in the regions where there are few samples the fit returns to the mean (in this case the PMV). As can be seen, for this user these models predict that their vote will exceed the PMV when the environment is too warm, and is approximately equal to the PMV when the environment is too cold.

The *cross-over point* is the point where a user is said to be comfortable, i.e. when their vote is zero. The estimated cross-over points are shown in Figures 7(b,e,h) with a cross and in Figures 7(c,f,i) with a white line. It is interesting to

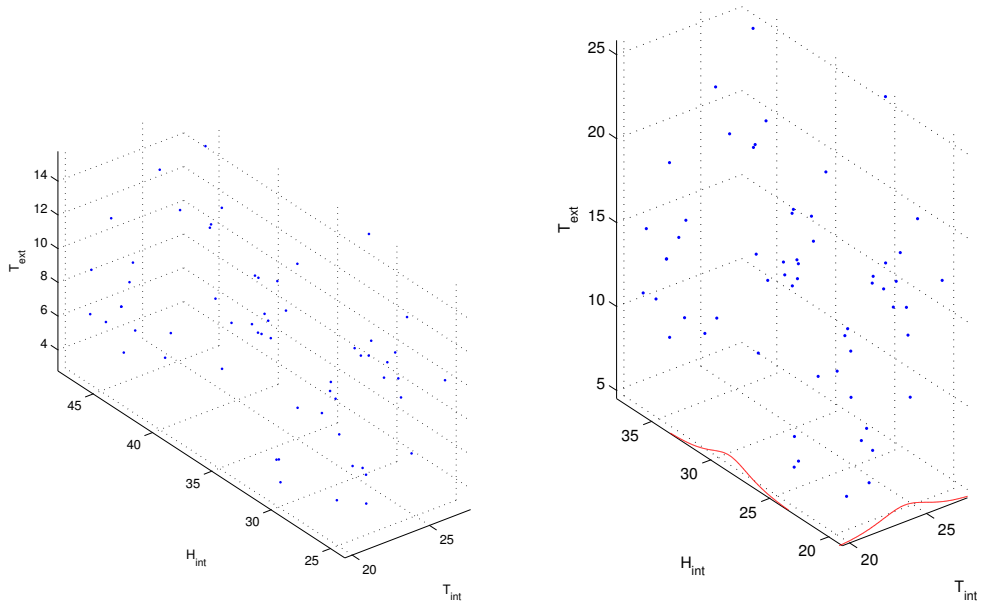

(a)

(b) Kernels shown in red. ($m_{t_{ext}} = 2.68, m_{h_{int}} = 0.62$)

Figure 6: Input data space: (a) Original (b) Scaled (note all axis scales are equal, User 1, GP1.)

note that GP1 deviates significantly from the PMV estimate (see Section 5.3 for specifics of PMV calculations) while GP2 and GP3 broadly agree. However, GP2 and GP3 disagree with the PMV when the humidity is to high (∼40%) or too low (∼25%). As Ireland has a temperature oceanic climate, humidity is liable to change and can be a major factor for a comfortable office environment. The fits indicate that the PMV cross-over estimate differs anywhere from 0.5° to 1.5° for this user. Overall, these fits demonstrate that the PMV is a good average indicator but that for a particular individual their preference can be biased in whole regions of the input space. The fits obtained using GP2 and GP3 are preferable to GP1 in the sense that in regions where the number of samples is low the estimate regresses to a reasonable value (the PMV) and not zero. Before examining the predictive power of the models we next examine outlier rejection.

5.2.2. Outlier influence reduction.

Figure 8 shows three panels which correspond to three rounds of variance reduction. In the first panel, on the left, we can see the GP1 model fit to the data with respect to the internal temperature and internal humidity. This user (different from that presented above) has been chosen as there is a large outlier; which is shown in red. The response for this outlier, Y_x, was zero at an internal temperature of 26°C and 35% humidity. The typical response for this user at that environmental setting is ≈2.5 and so this is an obvious outlier. The leverage exerted by this outlier is such that the response curve in this region (≈ 1.5 to 2) is well below the level it should be (about 2.5). As can be seen over the three rounds of outlier influence reduction the fit approaches the swarm of non-outlier data.

Table 2 shows how this reduction is achieved in detail by showing a sample of the values for ζ_x^i over three iterations. ζ_x^0, the initial guess, is set equal to 0.2256. The obvious outlier indicated in Figure 8 is datapoint 29; indicated in bold in the table. After the first iteration most of the variance estimates increase rapidly (reflecting a bad fit in general with the average standard deviation being 0.9418). The resulting fit in Figure 8c shows an improvement with the 'bowl' moving downwards towards the cloud at 2.5. The leverage of point 29 has thus been reduced. For the second iteration the variance estimates decrease for most of the points but increases for point 29. This reflects the fact that point 29 is further from the second round fit. Thus the overall effect is that during the first iteration a realistic estimate of the variance is produced (based on the initial guess) and then this estimate is refined in subsequent iterations. This also

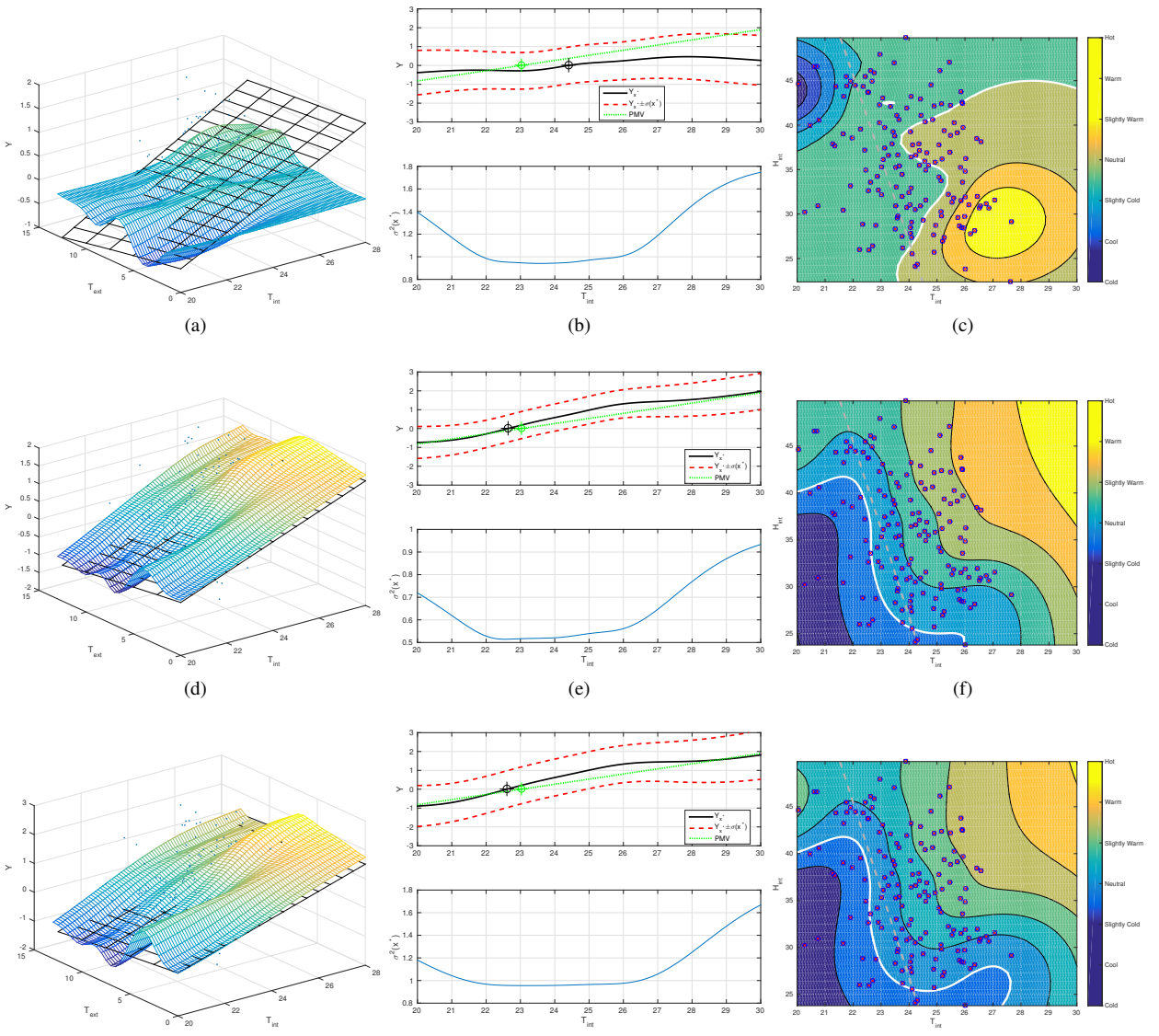

(a) (b) (c)

(d) (e) (f)

(g) Humidity = 36.2%, grid shows the PMV. (h) Humidity = 36.2%, T_{ext} = 8.86°C (i) T_{ext} = 8.86°C, white line shows $\hat{Y}(x) = 0$, dashed line shows PMV=0.

Figure 7: The response of models GP1 (row 1), GP2 (row 2) and GP3 (row 3) for User 1: Column 1 (a,d,g) response versus internal and external temperature (Humidity held constant), Column 2 shows the response wrt internal temperature (humidity and external temperature held constant), and column 3 shows the response with respect to internal temperature and internal humidity (external temperature held constant.) .

results in the leverage of outliers being reduced via increasing their measurement error variance estimates. Outlier rejection for models GP2 and GP3 works in an identical manner and is not shown for brevity.

5.3. Group results.

The first question we address here is the predictive performance of the GP's in general. In order to compare the performances we remove 5 test points from the data, train the GP's on the remaining points, and use these to predict the test points. This is bootstrapped over 50 runs with the training sets chosen uniformly at random each time. These results are compared with a multivariate (MV) linear model, a robust multivariate (rMV) linear model and the PMV

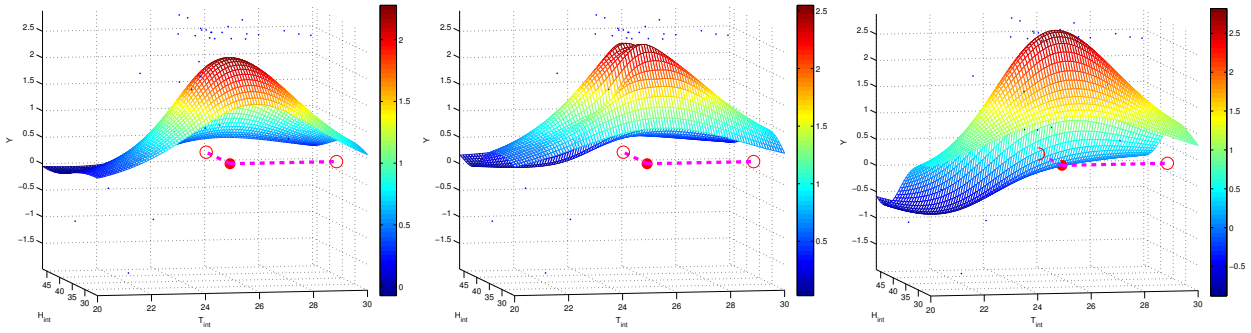

(a) Iteration 1. (b) Iteration 2. (c) Iteration 3.

Figure 8: The figures shows the GP model fitted to the responses from a user who is mostly too hot. a) The initial GP fit. b) the GP fit after the first round of outlier influence reduction c) the GP after the second round of outlier influence reduction. (The outlier is the large red dot in the centre of the figure with guides to the Y-Z and X-Z axis to allow perspective. The cloud of data points above the bowl occur at approx. $Y_x = 2.5$.)

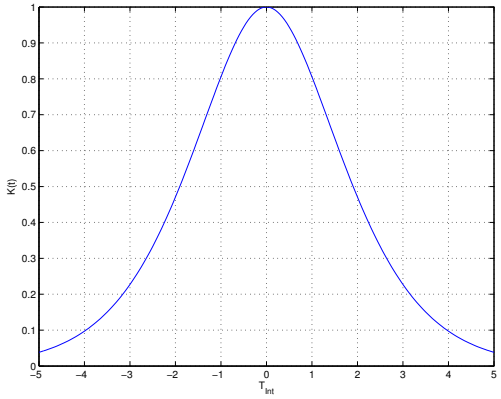

Figure 9: The Kernel function for the first user (in units of internal temperature).$\{\theta = 2.91, \nu = 2.54\}$

Data point	ζ_x^0	ζ_x^1	ζ_x^2	ζ_x^3
20	0.2256	1.1008	0.5221	0.3457
21	0.2256	0.2423	0.1334	0.0661
22	0.2256	1.6108	1.0503	0.7116
23	0.2256	1.1785	0.6708	0.2487
24	0.2256	0.8381	0.1921	0.0197
25	0.2256	0.8494	0.3860	0.1777
26	0.2256	0.3589	0.3462	0.1601
27	0.2256	1.3702	0.9884	0.7569
28	0.2256	0.6706	0.0603	0.0103
29	**0.2256**	**1.1982**	**1.2054**	**1.2276**
μ	0.2256	0.9418	0.5555	0.3724

Table 2: A selection of measurement error variance estimates over three iterations.

estimate based on the standard Irish PMV values.[15] Figure 10a shows the resulting root mean squared error (RMSE) for all 78 users. In all cases GP1 out-performs the PMV and the multivariate models thus validating this technique for thermal preference prediction. Table 3 shows a summary of the predictive statistics for all the models. The results show that the GP models empirically out perform the PMV significantly. The root mean squared error (RMSE) for the GP's is in the region of 0.71 while for the PMV it is 0.96 (averaged over all users). The standard deviation (STD) of the RMSE across users measures how variable the prediction accuracy is from user to user. As can be seen the PMV has a higher variation (i.e. the prediction RMSE reported, 0.96, is more variable compared to the GP models). The percentage signed error (PSE) is the percentage of predictions with the same sign as the observed value.[16] The results show that the GP models predict the correct direction $\sim$ 65 % of the time while the PMV is correct $\sim$ 50 % of the time which is equivalent to a random guess.[17] Between the GP models there is no clear winner. GP3 has the lowest reported RMSE but the difference between the RMSE's is not significant (as can be seen from the STD's). GP2 has the highest PSE but again the difference is not significant. The Log likelihood's show that GP2 explains the

[15]The standard PMV values for Ireland are: $T_{ext} = 12.8$, $H_{int} = 50\%$, Winter Clothing Level 0.85 clo, Activity Level: 1.2 met, Air Speed: 0.15 m/s, Humidity: 50%; note that the PMV is a non-linear function but is essentially linear in this range. An online PMV calculator may be found at **www.lth.se/fileadmin/eat/Termisk_miljoe/PMV-PPD.html**

[16]This is important from the control systems point of view as we often wish to know if the temperature should be either increased or decreased.

[17]This may be a remnant of the fact that the control systems are seeking to achieve setpoints derived from the PMV which would ideally result in votes hovering around zero.

Model	RMSE	STD	PSE	L
GP1	**0.7117**	0.29	**34.10**	57.3
GP2	0.7132	**0.28**	34.4	**61.6**
GP3	0.7141	0.28	34.16	54.3
MV	0.8273	0.35	38.25	-
rMV	0.8380	0.36	37.61	-
PMV	0.9600	0.41	49.61	-

Table 3: Summary of Predictive accuracy of the candidate models.

observations better than the other models but the likelihood ratios are almost 1 and so we cannot conclude that any of the candidate models is superior to the others. In summary using a GP which deviates from the PMV and includes an offset neither increases or decreases prediction accuracy (it is likely that the extra complexity involved in the models offsets the gains achieved).

The PMV is an estimate of the average human beings response. In this vein we take all the polls and fit a GP1 type model (i.e. using the sample population) to get an estimate of the population average. Figure 10b shows the resulting GP estimate. As can be seen there is in fact good correspondence between the two approaches at 18°C and 25°C. However, between these temperatures the GP estimate suggests a population preference function which changes more rapidly around the cross-over temperature (21°C). It would also appear that the PMV overestimates the cross-over temperature for this population at 22°C. Note that similar biases in the PMV have been observed in other studies such as [42].

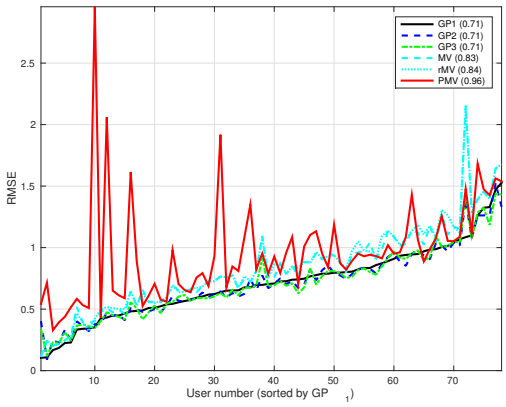

(a) Results for all users, bootstrapped over 50 runs, 5 randomly chosen samples are excluded from the training set and used for evaluation. (average RMSE in brackets)

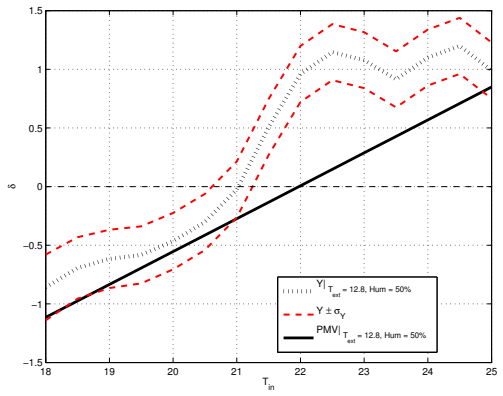

(b) The operating points used are the standard PMV Winter values for Ireland.

Figure 10: Comparing the GP and PMV: (a) Preference prediction RMSE (b) Response curve of a GP trained using all user data.

Next we examined the cross-over temperature for groups of individuals. For this we pooled the polls from N_p individuals, fitted a GP1 type model and noted the cross-over temperatures at the standard Irish Winter values. N_p was varied from 1 to 20 with 50 runs chosen randomly (so for N_p=1 there were repeated samples). Figure 12 shows the results of these simulations. As can be seen the PMV is again biased. The variance falls as the number of individuals' polls are pooled and we can expect individuals to have a crossover point between 18 and 22°C for small groups. However, with 20 individuals pooled the cross-over point can still vary significantly; from 20°C to 21.8°C.

Table 4 shows parameter and hyperparameter estimates along with the number of samples for the control group. Comparing the value of n to $\hat{\sigma_x}$ (the variance of the process) shows that as the number of data points increases the fit becomes smoother as expected. Note that this need not necessarily be the case; $\hat{\sigma}_x$ is not just a measure of the number of responses but also the *quality* of those responses. For example, a user might return many responses but with high

User	$\hat{\theta}$	$\hat{\nu}$	$\hat{m}_{T_{ext}}$	$\hat{m}_{H_{int}}$	$\hat{\sigma}_x$	$\hat{\mu}_x$	n
1	2.53	0.85	0.39	2.71	0.12	-9.43	61
2	4.97	2.79	0.13	2.01	0.21	-8.32	29
3	4.64	2.78	0.16	2.27	0.10	-19.43	48
4	5.00	2.26	0.11	2.18	0.72	-1.52	14

Table 4: Statistics for the control group of users.

measurement error variance (i.e. they just click in a random location out of complacency). This would be reflected in a higher $\hat{\sigma}_x$. $\hat{\mu}_x$ is negative for all users indicating that the room is in general too hot for the group as a whole. The estimated hyperparameters for users 2 to 4 shows surprising consistency with $\hat{\theta} \approx 5$, $\hat{\nu} \approx 2.7$, $\hat{m}_2 \approx 0.13$ and $\hat{m}_3 \approx 2$, as now discussed.

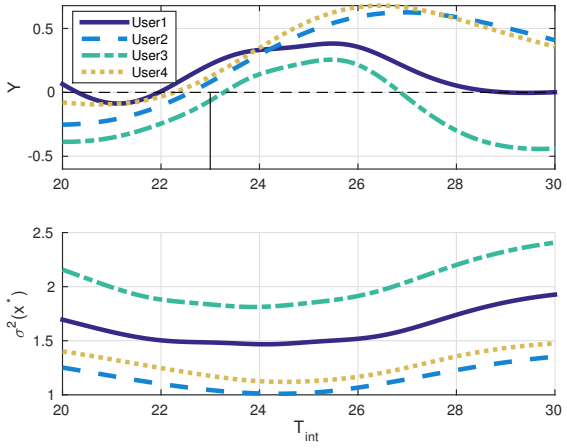

(a) The response curve from the 4 control group users with respect to internal temperature. (the external temperature is held constant at the average 11°C. The internal humidity is likewise held constant at the average, 39%. The line on the upper panel at 23°C corresponds to the temperature used in (b).)

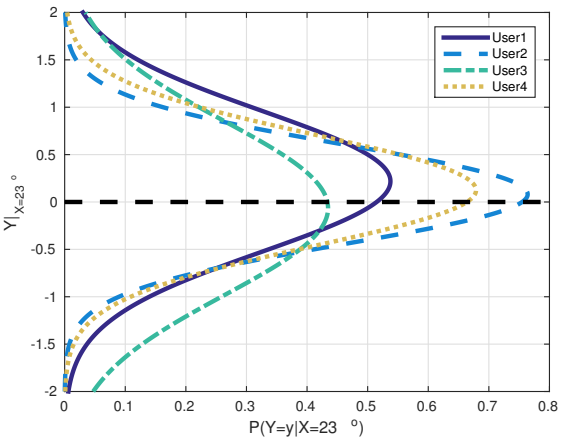

(b) The distributions of the response at 23°C for the 4 users. ($T_{ext} = 11°C$, $H_{int} = 39\%$. Note that this figure shows probability distributions on their side which is the conventional representation for a GP.

Figure 11: Comparing the response of 4 users (a) Response curves (b) Distribution of estimates around 23°C.

Next we examine if the quality of responses has changes over time (due to user fatigue with the application). Alternatively, we may instead ask how well the samples fit with the model over time, and this information is available in the model, specifically ζ_x. For this test we use the estimated noise variance of the samples, ζ_x, which we average across all users and segment by the number of days since the user started using the application. Figure 13 shows the expected noise variance of a sample taken in a user after using the application for x days. Also shown is a regression line which has a small positive slope. However, for the slope we cannot reject the null hypothesis (at a 10% level) as the p-value is 0.11. On balance, the data empirically indicates the responses degrade slightly over time.

For the NUIG dataset we present the results for one of the postgrad rooms showing the geographic distribution of preferences for the occupants. Figures 14 and 15 shows the mean estimate, μ_x and variance estimate, σ_x^2 for GP1 for each of the 26 occupants in this room. The figures shows that there is one individual on the western side (the y-axis) of the building who is persistently too hot while overall the other participants have a mean vote of zero. The variance shows that many of the participants in the western end of the room have a higher σ_x^2 than those in the rest of the room. The western side of this room is located above a server room, and in addition has a southern and a western facing window.

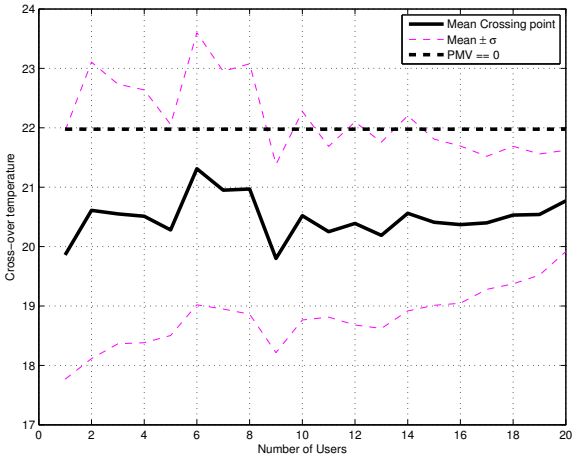

Figure 12: The cross-over values for combinations of users. The values shown are averaged over 50 runs with the users to be combined chosen independently.)

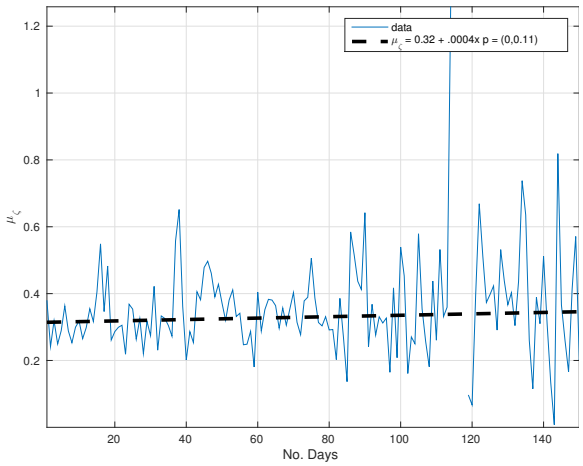

Figure 13: The estimated noise variance of the samples with the number of days the participant has used the application.)

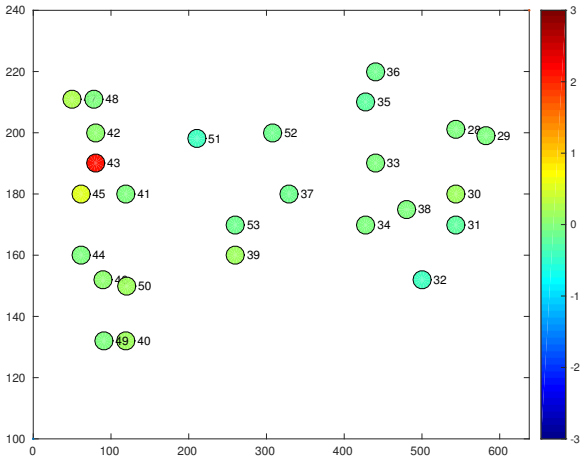

Figure 14: μ_x for the participants in a postgrad room at NUIG.)

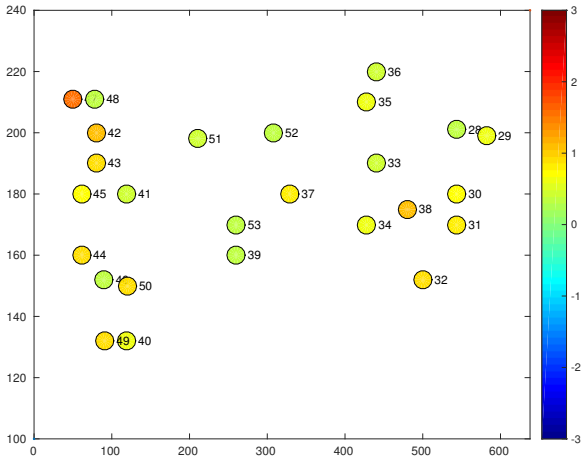

Figure 15: σ_x for the participants in a postgrad room at NUIG.)

5.3.1. Global priors

To examine the distribution of the hyperparameters the models from all 25 users were collected together and the distribution of the hyperparameter estimates from *all* users were examined to form *global* priors. These are shown in Figure 16. While some outliers do exist (such as user 1 above) the distributions in Figure 16 are concentrated about their respective maxima. In addition, the distributions for each of the candidate models broadly agree with GP3 showing the greatest concentration. Specifically the maxima (for GP1) in Figure 16 are $\{\bar{\theta}, \bar{\nu}, \bar{m}_{T_{ext}}, \bar{m}_{H_{int}}, \bar{\sigma}_x\} = \{4.91, 2.20, 0.63, 0.89, 0.24\}$. The maxima for Δ (this parameter is only present in GP3) is $\bar{\Delta} = \{0.05\}$. Collectively, this suggests that the application of GP's to preference modelling is a CIHM as described in the paper of Cass and Steffy [22] and this is a very useful result in several ways. First, there are physical interpretations for each parameter; $\bar{\theta}$ indicates that a poll taken at one point has an effective radius of 4.9° C (see Conclusion). The scaling between internal and external temperatures is 0.63 and the variance of the 'preference process' is smooth at 0.24. The variance of the GP estimates, $\bar{\sigma}_x$, is typically in the region of 1. This can be useful as an error identification and users which have an excessive value may not be using the interface correctly or it may point to an error in the measurement equipment. The prior for $\bar{\Delta} = \{0.05\}$ again demonstrates that the PMV is biased for most users. Secondly, these global priors can be used as priors for a new user in order to give a reasonable fit before a significant amount of data has been collected (as will be used later, in Section 5.4). Finally, we note that an alternative to using the maximum likelihood approach from Equation 6 the priors can be used to average across all possible values producing a more stable result.

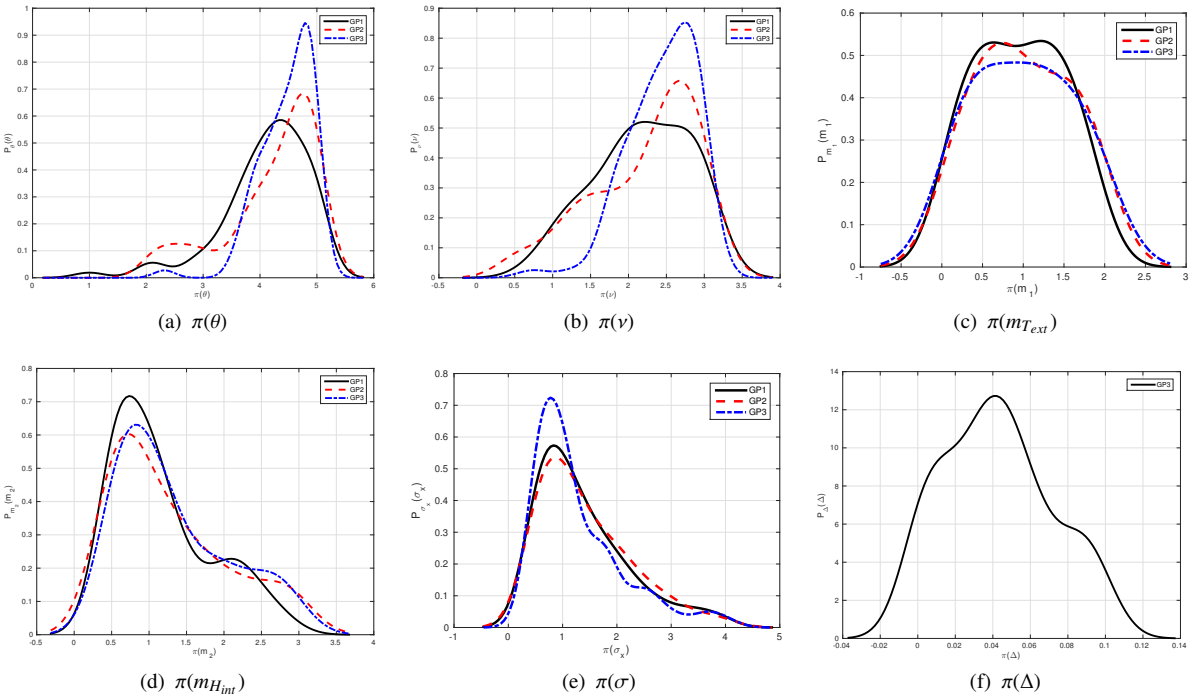

(a) $\pi(\theta)$ (b) $\pi(\nu)$ (c) $\pi(m_{T_{ext}})$

(d) $\pi(m_{H_{int}})$ (e) $\pi(\sigma)$ (f) $\pi(\Delta)$

Figure 16: Global prior distributions for the hyperparameters.

5.3.2. Combining Preference Functions

It is quite common that multiple people share an office space leading to the need for combined preferences (this Section deals specifically with *C***5**). In combining user preferences there are several factors that need to be considered. The first is *fairness*; each users opinion should count equally. However, this is tempered by two other closely related factors; how well do we actually know a users opinion? what should we do about users whose responses are

conflictual?[18] Combining these factors can be done quite naturally given the Gaussian Process (here we use GP1) representation of the process. Figure 17a shows the response curves for the 4 users in the control group. In addition, the value of $\hat{\sigma}^2(x^*)$ at the internal temperatures, x^*, are shown in the lower panel. The points at which $\hat{Y}_{x^*} = 0$ (the cross-over points) for the four users are $\{22.9°, 22.5°, 23.6°, 20.3°\}$, respectively. Thus the average cross-over point is $22.3°C$. However, this figure does not take into account that our confidence about each user differs significantly as can be seen on the lower panel of Figure 17a. User three has a significantly higher variance, $\hat{\sigma}^2(x^*)$, than all the others, while user two has the lowest variance and thus we are more confident of that response. A consistent weighting of the user responses is thus required.

At this stage it is useful to consider more rigorously the optimisation criteria. Given a particular environment we would like to know how likely it is that the users are unhappy. Equivalently, we can ask how likely it is that they are happy. Estimates are readily available from the GP models and an example is shown with the aid of Figure 17b. This Figure shows the predictive distributions of the responses at 23°C. The data in this figure refers to just one operating point; the internal temperature at 23°C (the other variables being set to the average). Comparing Figures 17a and 17b it can be seen that User three, for example, has a mean response ($\hat{Y}_{x^*}$) of -0.27 at 23°C and in Figure 17b it can be seen that the distribution ($\sim \mathcal{N}\{\hat{Y}_{x^*}, \hat{\sigma}^2(x^*)\}$) around this response is wider than for the other users (i.e. there is greater uncertainty). One way of combining preferences while taking this uncertainty into account is to estimate the expected number of neutral votes as:

$$J_1(x^*) = \frac{1}{4}\sum_{i=1}^{4} P_i(Y_{x^*} = 0|x = x^*) \tag{14}$$

where $P_i(Y_{x^*} = 0|x = x^*)$ is the PDF of the response for the i^{th} user evaluated at zero and $J_1(x^*)$ is the name given to this combination function.

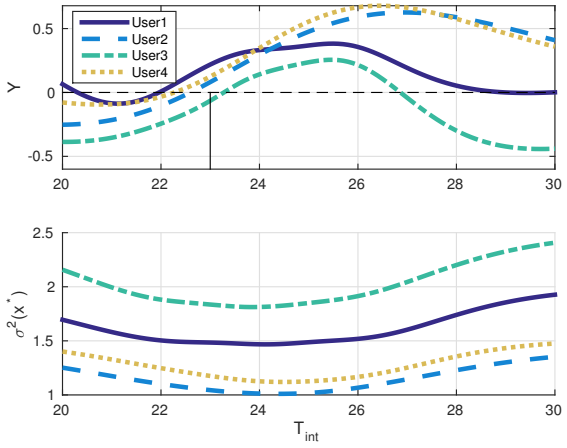

(a) The response curve from the 4 control group users with respect to internal temperature. (the external temperature is held constant at the average 11°C. The internal humidity is likewise held constant at the average, 39%. The line on the upper panel at 23°C corresponds to the temperature used in (b).)

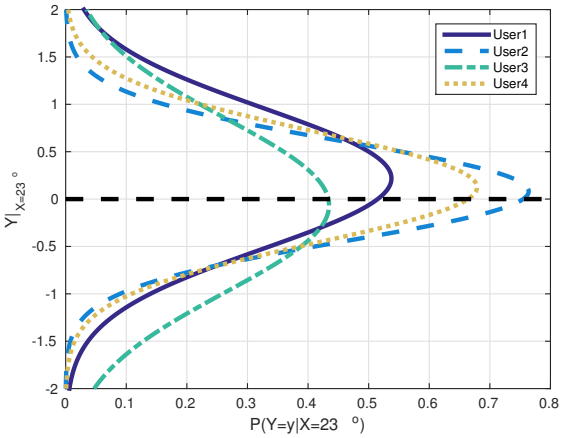

(b) The distributions of the response at 23°C for the 4 users. ($T_{ext} = 11°C$, $H_{int} = 39\%$. Note that this figure shows probability distributions on their side which is the conventional representation for a GP.

Figure 17: Comparing the response of 4 users (a) Response curves (b) Distribution of estimates around 23°C.

Figure 18a shows the value of $J_1(x^*)$ corresponding to the response curves in Figure 17a. The individual contributions to this value from the four users are also shown. As can be seen, $J_1(x^*)$, reaches a maximum at 22.8°C compared with the 22.3°C derived from the average vote. Alternative strategies for combining the votes can be imagined and

[18] In the sense that one response might indicate that the user is too cold at 23°C while another indicates that they are too hot; all things being equal.

tailored to the preference of the building manager. Note that the choice of metric is subjective. So, for example, a manager who wishes to reweight the functions such that each has the same average weighting can weight each user by their process variance before combining as:

$$J_2(x^*) = \frac{1}{4}\sum_{i=1}^{4}\frac{1}{\hat{\sigma}^2_{x_i}}P_i(Y_{x^*} = 0|x = x^*) \tag{15}$$

where $\hat{\sigma}^2_{x_i}$ is the process variance with the subscript added to the notation to denote the i^{th} user (Equation 11). The effect of this combining strategy is to give each user the same overall variance and thus influence. This influence can still be stronger in some regions as $\hat{\sigma}^2(x^*)$ is a function of x. Alternatively, we might be interested in minimising the absolute expected vote, a strategy that takes into account not just the probability that a user is happy but also *how unhappy* they might be:[19]

$$J_3(x^*) = -\frac{1}{4}\sum_{i=1}^{4}\int_{y=-3}^{y=3}|y|P_i(Y_{x^*} = y|x = x^*)dy \tag{16}$$

Additionally, we may wish to bias the combination towards very unhappy users by using the square of the vote as the core of the metric as:

$$J_4(x^*) = -\frac{1}{4}\sum_{i=1}^{4}\int_{y=-3}^{y=3}y^2P_i(Y_{x^*} = y|x = x^*)dy \tag{17}$$

The resulting values are shown normalised for comparison in Figure 18b (as we are interested in the shape and not the amplitude). These maxima occur at {22.8,22.9,22.3,22.5}° C , respectively. The cost functions in this figure are well behaved in terms of being used as control signals; they have a maximum and they fall away from that maximum smoothly without discontinuities.[20]

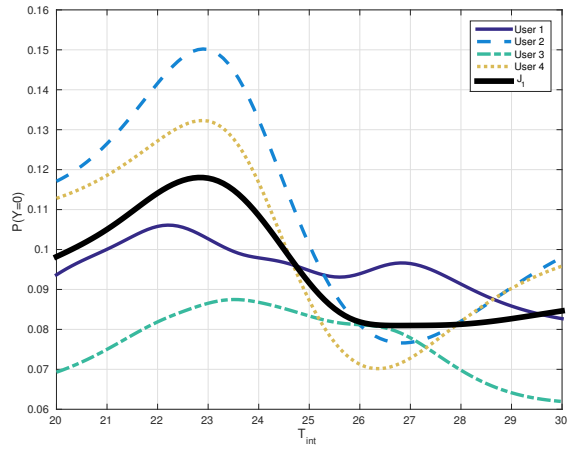

(a) The probability of a neutral response for four users and the resulting combination under strategy $J_1(x^*)$.

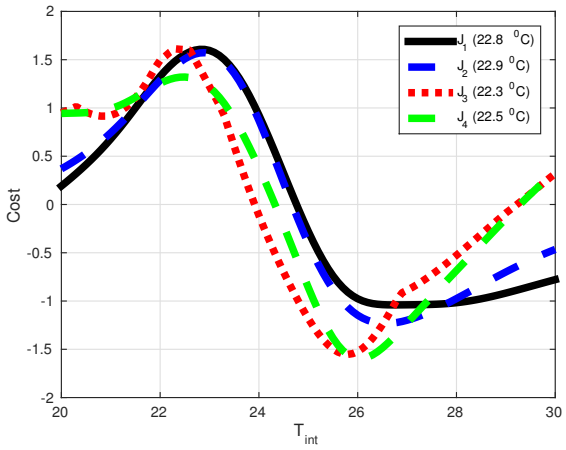

(b) Four different combination strategies (y-axis is normalised, appropriate function extrema in brackets).

Figure 18: Comparing the combination of 4 users (a) $J_1(x^*)$ and constituent preferences (b) $J_1(x^*)$, $J_2(x^*)$, $J_3(x^*)$, and $J_4(x^*)$. ($T_{ext} = 11°C, H_{int} = 39\%$)

Figure 19 shows a mesh plot of the combination functions with respect to internal and external temperature. While J1 and J2 are monotonic, smooth and well behaved J3 and J4 may cause problems for a control system as they contain local maxima and minima (these occur around the preferred environment of individual users). In selecting the combination function care should thus be taken that the resulting function does not default to a single users preferences.

[19] We insert a minus here for convenience so that all combination functions are to be maximised.

[20] The exception are the tails at the extremity (30 °C) which occur because of the lack of data at that point; causing $\hat{Y}_30$ to return to zero as mentioned in Section 5.2.1; note this can easily be removed using a sanity check.

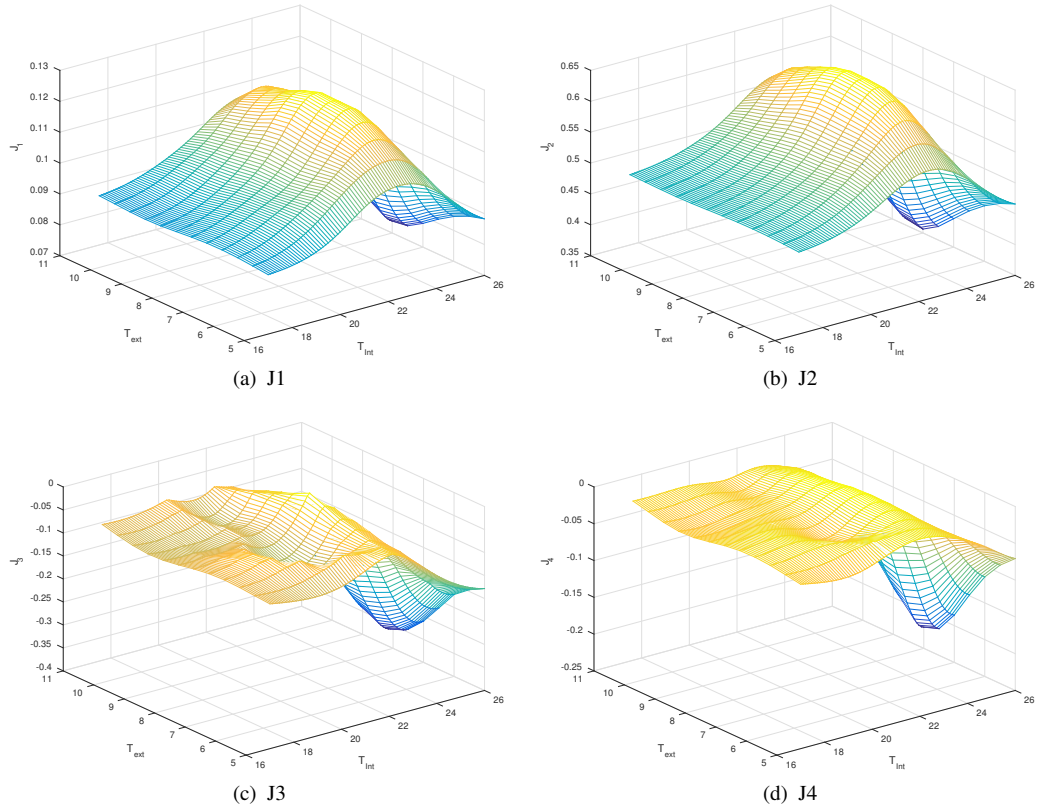

(a) J1 (b) J2

(c) J3 (d) J4

Figure 19: The combination of four users' preferences, using 4 different strategies (humidity kept constant at 39%).

5.4. Active learning.

Up to this point we have been discussing preference functions and characteristics of the data. We now turn our attention to efficient means of collecting that data, i.e. active learning. This Section presents the results of the active learning algorithm over time and attempts to give an empirical measure of the improvement over random sampling of this technique. To begin, Figure 20a illustrates two paths[21] through the input space traversed in two different days; one in February and the other in May. The day in February was more humid than that in May and surprisingly the May day was colder than February in the morning but heated up throughout the day ending at about 12°C outside. The aim of the active learning section is to determine the best point during the path to take a sample (given the samples already taken).

Figure 20b shows the expected return, $\sigma^2_{x^*}$ for the two example paths shown in Figure 20a.[22] As can be seen the optimal times to sample for these two days are 11:15am and 6pm (for the February and May day respectively). The following intuitive explanation can be given; for the May day, the path proceeds through well known territory but ends with a high external temperature and high internal temperature which correspond to a region of the input space which has not previously been sampled. Conversely, the start of the February path occurs in a region of the input space that has not previously been sampled. It is also satisfying to note that there is a large variation in the expected return during the day (from $\sim$ 4,000 to 7,000). Were we to sample at 3pm in the May day then the resulting information returned is quite low.

Active sampling is normally compared with grid sampling and random sampling. In the current setting grid sampling is not possible as we have no control over the weather. In reality, we cannot both randomly sample *and*

[21] A path is how the environment changes over the course of a day.

[22] It is assumed we know or can predict the path taken during the day. Weather and heating system prediction is however beyond the scope of this paper.

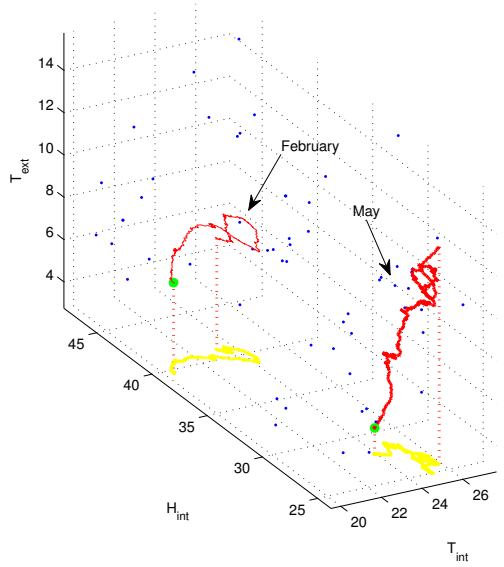

(a) The path starts at 8am (green dot) and ends at 6pm. (The shadow of the path is shown in yellow to help with perspective).

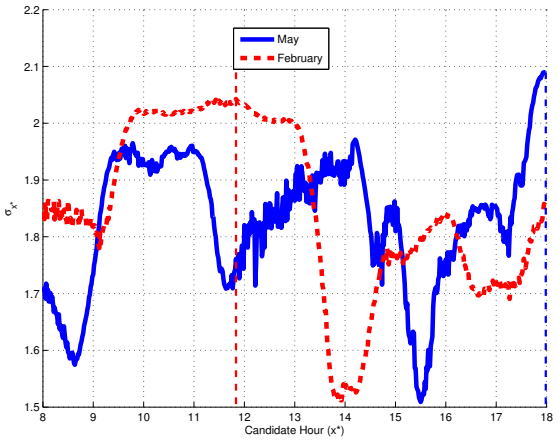

(b) The expected returns along the paths shown in Figure 20a.

Figure 20: Sample paths in the input space (a) examples of how the inputs change over the day (winter and summer) (b) the expected return along those paths.

actively sample. Fortunately, we have many users and the study was carried out for a long period. Therefore, we have a good idea of users' preference functions and associated sampling error statistics. This allows us to use GP1 fitted on *all* the data to *simulate* a sample of users' preference functions under different conditions. In addition to investigating active sampling, we also investigate the integration of prior information into the models. There are two pieces of prior information that we have and investigate. The first is that all users share a global prior over their hyper-parameters (Section 5.3.1) and this can be used as the starting value for the hyper-parameter estimates. The second piece of prior information is that all humans are unhappy in extreme environments. These may be included in the GP simply as manually inserted sample points with maximal responses, we call these the *boundary points*. The boundary points used are (subjectively) derived from the PPD. It was assumed that a PPD level of 70% and above constituted an area of definite unhappiness. Thus we chose to randomly search for points where the PPD = 70%. Figure 21 shows several hundred such points in the input space. 33 of these are chosen at random and their corresponding y-values are set at +3 or -3.[23]

Putting the above together we have 6 scenarios to investigate using a mix of sampling and prior information:

(*i*) Random sampling,

(*ii*) Random sampling with the global prior provided,

(*iii*) Random sampling with the global prior and boundary points provided,

(*iv*) Active sampling,

(*v*) Active sampling with the global prior provided, and

(*vi*) Active sampling with the global prior and boundary points provided.

[23] 33 is chosen subjectively, we didn't want too many points as this would slow down the algorithm and they would dominate.

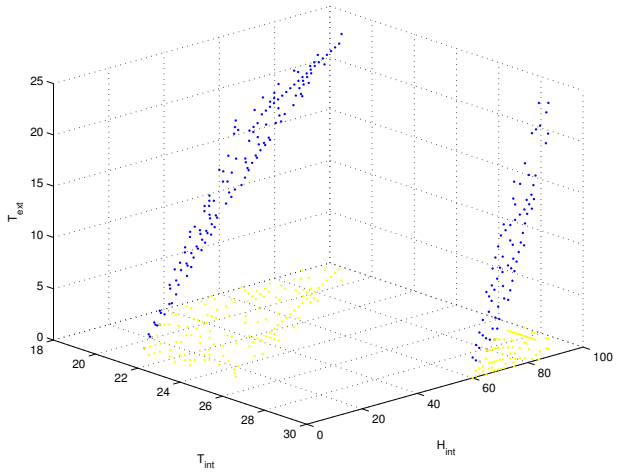

Figure 21: The boundary points; each point occurs when the PPD is at 70%. The shadow of the points is shown in yellow to help with perspective.

Finally, the simulations are evaluated using the Sum Square Error (SSE) between the GP function based on all the data actually collected and that created by the data collected in simulations (i)-(vi), above. Figure 22 shows the results for these three strategies for four different users. In order to account for random conditions (such as the path taken on a particular day) the simulations are conducted thirty times and the average is presented. As can be seen the results are mixed. At first there seems to be little difference between the active learning (i) and random sampling (iv) results. This is surprising, but is due to the fact that when few samples are present any sample will provide roughly the same amount of information. Including the global prior results in an improved estimate in all cases. This result is encouraging as it demonstrates the use of the global prior and in addition empirically suggests that it is useful for the average human being. The active learning with global prior (v) is superior to the random sampling with global prior (ii) but only marginally, although the result holds for all the users. Finally, inclusion of the global prior and the boundary conditions provides the best result. This shows that including the known information greatly increases the speed at which the user function is learned. Approach (vi) shows a definite improvement over approach (iii) (the approaches differ only in active versus random sampling). However, following the collection of approximately 15 samples, it can be seen that approaches (vi) and (iii) start to drift upward again. The cause of this is that the collected samples now start to differ from the boundary. This implies that the boundary points should be discounted as we collect more samples (or even jettisoned). Putting these results together suggests the data collection scenario vi) which is repeated as an algorithm 1 below.

6. Conclusions and Future Work

The aim of this paper was to show that a ubiquitous unobtrusive preference collection sample could be used to estimate an individuals preference function. While we found that this is the case, it does require strategies to deal with several data artefacts; outliers and a deadband. We found from talking with the participants that the feedback was generally positive and the intrusion caused by the interface was minimal. It is interesting to note that clicking outside the validation lines was not used (by anyone) perhaps because to use them would have required the users attention. Alternatively, an aversion by users to a negative response (i.e. to indicate that they didn't want to answer the poll) might explain this (note that this feature was demonstrated to every user). Instead, the deadband seems to have become the location for preferences given without thought.

Empirical evidence in this paper suggest that the preference function is a CIHM. The global priors apart from being useful as an initial estimate of a users hyperparameters may also be useful for compressed sensing. One can imagine a temperature sensor only transmitting changes in temperature that are significant to the estimate of a users preference thus saving power.

The regression technique used to process the data, i.e. a Gaussian Process, was involved (i.e. complex) but was chosen for a reason; *flexibility*. The GP framework allows for active learning, taking into account prior information

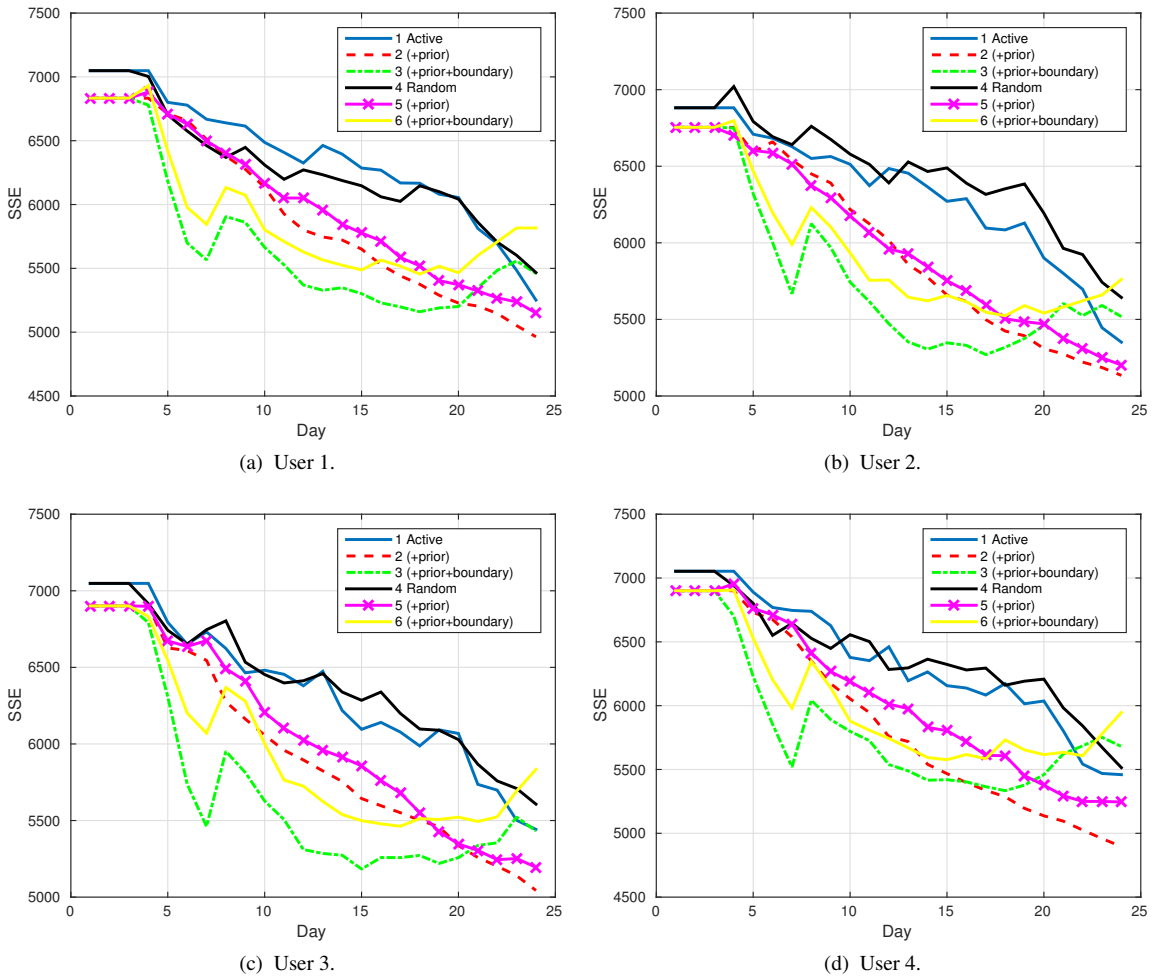

(a) User 1. (b) User 2.

(c) User 3. (d) User 4.

Figure 22: Comparing the performance of different strategies for three users.(Results are averaged over 30 runs)

(global priors and boundary conditions) as well as allowing a natural combination of users preference functions. The three different GP models tested showed excellent response to the data with GP2 perhaps being preferable for aesthetic reasons (as predictions outside the sampling region will regress to the PMV). Non-stationary GP's, in which the kernel is allowed to vary across the input space, are also of future interest reflecting that at different environmental settings our reaction may be different. One particular type of non-stationary GP, the treed Gaussian process, has a finite set of kernel functions with a boundary defining what part of the input space is assigned each kernel. This could be interesting for preference modeling because humans react differently to cold and hot environments [41] and a different kernel might be appropriate for each. A non-isotropic kernel may also be of interest but as mentioned in Section 4.3 we have no reason to suspect a more complex model and so opted not to. In the future we intend to apply active learning in a live setting but this requires a forecast of the weather and environmental settings in the room, an involved task in itself.

Future work will concentrate on integrating the preference and control. This is envisaged to be particularly interesting in the case of the NUIG site as the large elongated rooms contain ∼100 occupants. The elongated shape of the room allows for different control settings for each part, to a certain extent, and so the combination function would have to consider, in addition, the location of the participant.

In conclusion, fundamentally the approach taken above is to use a simple unobtrusive interface thus producing noisy data and then extract the required information later using advanced statistical techniques. In addition the Gaus-

Algorithm 1: Active learning with prior Information.

Data: Boundary points
Result: $\hat{Y}_{x^*}, \hat{\sigma}^2(x^*)$
begin
Initialise: Set hyperparameters to prior:
$\{\theta, \nu, m_{T_{ext}}, \sigma_x\} = \pi(\bar{\theta}, \bar{\nu}, \bar{m}_{T_{ext}}, \bar{\sigma}_x)$
Set samples to boundary conditions:
$x_{1:n} = \{x_{boundary}\}$
$y_{1:n} = \{y_{boundary}\} \in \{-3, 3\}$
for $i = 1 \rightarrow N$ **do**
Infill fn: Predict path for environment,
Use GP to estimate variance along path. (Eqn. 9)
Find time of max variance. (Sec. 4.4).
Sample: Sample at this time.
Model: Fit GP (Sec. 4.1).
Outlier rej: **for** $j = 1 \rightarrow 3$ **do**
Re-estimate variance (Sec. 4.2).
Fit GP

sian Process technique used is of interest in the general real-world sensing field as it allows several tasks beyond modelling to be achieved. Specifically, it is envisaged that these techniques will be found useful when modelling, sampling and understanding general human activities.

Acknowledgement

This work is funded by Science Foundation Ireland as part of the ITOBO project under grant No. 07.SRC.I1170. The authors would like to thank Robert Houghton and Richard Mortier at the University of Nottingham for their advice on human-computer interaction. We would also like to thank Daniel Coakley at NUIG for his assistance with the NUIG site data.

References

[1] L. Prez-Lombard, J. Ortiz, C. Pout, A review on buildings energy consumption information, Energy and Buildings 40 (2008) 394 – 398.
[2] Buildings energy data book, US Department of Energy (2010).
[3] M. Norkus, D. Fay, M. J. Murphy, F. Barry, G. OLaighin, L. Kilmartin, On the application of active learning and Gaussian processes in postcryopreservation cell membrane integrity experiments, IEEE/ACM Trans. Comput. Biol. Bioinformatics 9 (2012) 846–856.
[4] A. Ioannou, L. Itard, Energy performance and comfort in residential buildings: Sensitivity for building parameters and occupancy, Energy and Buildings 92 (2015) 216 – 233.
[5] A. H. yat Lam, Y. Yuan, D. Wang, An Occupant-participatory Approach for Thermal Comfort Enhancement and Energy Conservation in Buildings, in: Proceedings of the 5th International Conference on Future Energy Systems, e-Energy '14, ACM, New York, NY, USA, 2014, pp. 133–143.
[6] J. York, Humancomputer interaction issues for mobile computing in a variable work context, International Journal of Human-Computer Studies 60 (2004) 771–797.
[7] D. Fay, K. N. Brown, L. O'Toole, Lies, damn lies and preferences: A Gaussian process model for ubiquitous thermal preference trials, in: Proceedings of the Fourth ACM Workshop on Embedded Sensing Systems for Energy-Efficiency in Buildings, BuildSys '12, ACM, New York, NY, USA, 2012, pp. 184–191.
[8] R. Dedear, G. S. Brager, Developing an Adaptive Model of Thermal Comfort and Preference, ASHRAE Transactions 104 (1998).
[9] B. Moujalled, R. Cantin, G. Guarracino, Comparison of thermal comfort algorithms in naturally ventilated office buildings, Energy and Buildings 40 (2008) 2215 – 2223.
[10] P. Fanger, Thermal Comfort, Danish Technical Press, 1970.
[11] F. Jazizadeh, F. M. Marin, B. Becerik-Gerber, A thermal preference scale for personalized comfort profile identification via participatory sensing, Building and Environment 68 (2013) 140 – 149.

[12] A. K. Clear, J. Morley, M. Hazas, A. Friday, O. Bates, Understanding adaptive thermal comfort: New directions for ubicomp, in: Proceedings of the 2013 ACM International Joint Conference on Pervasive and Ubiquitous Computing, UbiComp '13, ACM, New York, NY, USA, 2013, pp. 113–122.
[13] W. P. Syed Ihtsham ul Haq Gilani, Muhammad Hammad Khan, Thermal comfort analysis of pmv model prediction in air conditioned and naturally ventilated buildings, Energy Procedia 75 (2015) 1373–1379.
[14] S. Wu, J.-Q. Sun, Two-stage regression model of thermal comfort in office buildings, Building and Environment 57 (2012) 88–96.
[15] J. A. Orosa, A new modelling methodology to control HVAC systems, Expert Syst. Appl. 38 (2011) 4505–4513.
[16] S. Atthajariyakul, T. Leephakpreeda, Neural computing thermal comfort index for HVAC systems, Energy Conversion and Management 46 (2005) 2553–2565.
[17] J. Langevin, J. Wen, P. L. Gurian, Modeling thermal comfort holistically: Bayesian estimation of thermal sensation, acceptability, and preference distributions for office building occupants, Building and Environment 69 (2013) 206 – 226.
[18] D. Daum, F. Haldi, N. Morel, A personalized measure of thermal comfort for building controls, Building and Environment 46 (2011) 3–11.
[19] V. L. Erickson, A. E. Cerpa, Thermovote: Participatory sensing for efficient building HVAC conditioning, in: Proceedings of the Fourth ACM Workshop on Embedded Sensing Systems for Energy-Efficiency in Buildings, BuildSys '12, ACM, New York, NY, USA, 2012, pp. 9–16.
[20] Z. Song, L. Wang, Y. Lu, Social learning soft thermostat for commercial buildings, in: Proceedings of the Fourth ACM Workshop on Embedded Sensing Systems for Energy-Efficiency in Buildings, BuildSys '12, ACM, New York, NY, USA, 2012, pp. 199–200.
[21] Q. Zhao, Z. Cheng, F. Wang, Z. Chen, Y. Jiang, Z. Zhong, Experimental assessment of a satisfaction based thermal comfort control for a group of occupants, in: IEEE International Conference on Automation Science and Engineering, CASE 2015, Gothenburg, Sweden, August 24-28, 2015, IEEE, 2015, pp. 15–20.
[22] R. E. Cass, D. Steffey, Approximate Bayesian inference in conditionally independent hierarchical models (parametric empirical Bayes models), Journal of the American Statistical Association 84 (1989) 717–726.
[23] E. C. M.M. A. Rahman, D. Huizenga, A low-cost intelligent thermostat incorporating a learning algorithm based scheduler and internet accessible control interfaces, in: Proceedings of the 2014 ASEE North Central Section Conference, ASEE, 2014.
[24] R. Martinez-Cantin, N. de Freitas, A. Doucet, J. Castellanos, Active Policy Learning for Robot Planning and Exploration under Uncertainty, The MIT Press, Cambridge, MA, pp. 321–328.
[25] J. Serradilla, J. Q. Shi, A. J. Morris, Fault detection based on Gaussian process latent variable models, Chemometrics and Intelligent Laboratory Systems (2011).
[26] T. Alpcan, A framework for optimization under limited information, in: Proceedings of the 5th International ICST Conference on Performance Evaluation Methodologies and Tools, VALUETOOLS '11, ICST (Institute for Computer Sciences, Social-Informatics and Telecommunications Engineering), ICST, Brussels, Belgium, Belgium, 2011, pp. 234–243.
[27] T. J. Santner, B. Williams, W. Notz, The Design and Analysis of Computer Experiments, Springer-Verlag, 2003.
[28] R. B. Gramacy, Bayesian treed Gaussian process models, PhD thesis, U.C. Santa Cruz, 2005.
[29] S. Seo, M. Wallat, T. Graepel, K. Obermayer, Gaussian process regression: Active data selection and test point rejection, in: DAGM-Symposium, pp. 27–34.
[30] C. E. Rasmussen, C. K. I. Williams, Gaussian Processes for Machine Learning, MIT press., 2006.
[31] P. W. Goldberg, C. K. I. Williams, C. M. Bishop, Regression with input-dependent noise: A Gaussian process treatment, in: NIPS, pp. 493–499.
[32] K. Kersting, C. Plagemann, P. Pfaff, W. Burgard, Most likely heteroskedastic Gaussian process regression, in: Z. Ghahramani (Ed.), Proceedings of the 24th Annual International Conference on Machine Learning (ICML 07), Corvallis, OR, USA, pp. 393–400.
[33] A. Krause, A. Singh, C. Guestrin, Near-optimal sensor placements in Gaussian processes: Theory, efficient algorithms and empirical studies, The Journal of Machine Learning Research 9 (2008) 235–284.
[34] M. A. Osborne, A. Rogers, S. Ramchurn, S. J. Roberts, N. R. Jennings, Towards real-time information processing of sensor network data using computationally efficient multi-output Gaussian processes, in: Proceedings of the 7th international conference on information processing in sensor networks, pp. 109–120.
[35] M. Osborne, Bayesian Gaussian Processes for Sequential Prediction, Optimisation and Quadrature, PhD thesis, University of Oxford, 2010.
[36] D. J. C. MacKay, Information-based objective functions for active data selection, Neural Computation 4 (1992) 589–603.
[37] D. A. Cohn, Neural network exploration using optimal experimental design, in: NIPS, pp. 679–686.
[38] M. Norkus, D. Fay, M. J. Murphy, F. Barry, G. OLaighin, L. Kilmartin, On the application of active learning and Gaussian processes in postcryopreservation cell membrane integrity experiments, IEEE/ACM Trans. Comput. Biol. Bioinformatics 9 (2012) 846–856.
[39] G. McLachlan, K. Basford, Mixture Models: Inference and Applications to Clustering, Marcel Dekker, New York, 1988.
[40] M. Orne, On the social psychology of the psychological experiment: With particular reference to demand characteristics and their implications., American Psychologist 17 (1962) 776–783.
[41] L. A. Jones, M. Berris, The psychophysics of temperature perception and thermal-interface design, in: Symposium on Haptic Interfaces for Virtual Environment and Teleoperator Systems 2002, pp. 137–137.
[42] C. Manna, N. Wilson, K. N. Brown, Personalized thermal comfort forecasting for smart buildings via locally weighted regression with adaptive bandwidth, in: SMARTGREEENS 2013, 2nd Intl Conf on Smart Grids and Green IT Systems.